Journal of Water Process Engineering 38 (2020) 101380

Contents lists available at ScienceDirect

Journal of Water Process Engineering

journal homepage: www.elsevier.com/locate/jwpe

Adsorption of endocrine disrupting compounds and other emerging contaminants using lignocellulosic biomass-derived porous carbons: A review

U.A. Qureshi[a], B.H. Hameed[b,*], M.J. Ahmed[c]

[a] Department of Chemistry, Government Boys Degree College, Qasimabad, Hyderabad, 71000, Pakistan
[b] Department of Chemical Engineering, College of Engineering, Qatar University, P.O. Box: 2713, Doha, Qatar
[c] Department of Chemical Engineering, Engineering College, Baghdad University, P.O. Box 47024, Aljadria, Baghdad, Iraq

ARTICLE INFO

Keywords:
Endocrine disrupting chemicals
Kinetics
Isotherm
Hydrothermal carbonization
Activated carbon
Emerging contaminants

ABSTRACT

Hydrochars from lignocellulose biomass have received an upsurge of interest in different fields, especially in the area of adsorption. Hydrothermally produced hydrochars are effective adsorbents for removing different pollutants, and they serve as a cheap and sustainable raw material for subsequent activation to achieve porous activated carbons (ACs) with large surface areas. In this review, recent studies on preparation and characteristics of adsorbents in terms of hydrochars from lignocellulose biomass and their derived ACs are presented and discussed. The application of these adsorbents for the removal of endocrine disrupting chemicals and other emerging pollutants is included. The sources and classification, adsorption isotherm, kinetics, and mechanism of these pollutants and the capability of regenerating and reusing cheap and efficient adsorbents such as hydrochar and ACs are also discussed. This review identifies knowledge gaps and proposes insights into new directions for improving the applications of hydrochar and ACs as adsorbents.

1. Introduction

Emerging contaminants (ECs) are recently discovered compounds and other materials that have long been existed in the environment but whose existence and influence are only now being identified. ECs include a wide group of contaminates, such as drugs and personal care products (PPCPs), herbicides, veterinary products (e.g., hormones), food additives, industrial compounds (e.g., metabolites and degradation products), and engineered nanomaterials. Studies have revealed that these ECs are frequently and abundantly found in wastewaters and surface water [1]. Another class of pollutants is referred to as endocrine disrupting compounds (EDCs), which are known to affect the endocrine system, including the growth and reproduction of humans and animals. Such compounds are widely used in industrial applications, cosmetics, and pharmaceuticals. These compounds may include some phenolic compounds, polyaromatic hydrocarbons, dioxins, natural steroidal estrogens, synthetic estrogens, and industrial chemicals [2]. Their concentrations in water bodies are high and thus cause many health-threatening problems. Therefore, the presence of such toxic pollutants requires the immediate development of effective treatment strategies to achieve a safe and green aqueous environment.

The control of environmental pollutants, namely, ECs and EDCs, from aqueous systems through the adsorption technique has received growing interest because it is simple and offers a wide variety of cheap and efficient adsorbent materials like hydrochars and their derived activated carbons (ACs). Hydrochar is a solid residue containing reduced hydrogen and oxygen contents from the hydrothermal carbonization (HTC) of biomaterials, particularly lignocellulose, in the presence of subcritical liquid water [3]. Unlike those from other biomass utilization techniques, such as pyrolysis, biological conversion, and densification to solid fuel, hydrothermal treatment-based hydrochar materials have drawn significant research interest due to their numerous advantages, such as low processing temperatures (180 °C – 250 °C), low ash contents, direct applicability to wet

Abbreviations: AC, activated carbon; AFEX, ammonia fiber explosion; BET, Bruneur Emmet Teller; DDT, 2,2-bis (p-chlorophenyl)ethane; DHT, dihydrotestosterone; E1, estrone; E2, 17β estradiol; E3, estriol; EC, emerging contaminants; EDC, endocrine disrupting compounds; FTIR, fourier transform infrared spectroscopy; HHV, high heating values; HTC, hydrothermal carbonization; HTL, hydrothermal liquifaction; MC, magnetic carbon composites; PAH, polyaromatic hydrocarbons; PP-HYD-ox/dorzo, oxidized activated carbon from potato peel hydrochars for dorzolamide; PP-HYD-ox/prami, oxidized activated carbon from potato peel hydrochars for pramipexole; PZC, point of zero electric charge; WWTP, waste water treatment plant

* Corresponding author.
E-mail address: b.hammadi@qu.edu.qa (B.H. Hameed).

https://doi.org/10.1016/j.jwpe.2020.101380
Received 2 March 2020; Received in revised form 16 May 2020; Accepted 18 May 2020
Available online 07 September 2020

feedstock, high product yield (30 wt%–60 wt%), and zero generation of hazardous chemical waste [4]. Other properties, such as porosity and variety of aliphatic and aromatic functional groups, place these materials at the forefront of certain applications, such as mitigating atmospheric CO_2, producing biofuel by curtailing the dependency on fossil fuels, energy storage, environmental pollution control, and soil amelioration [5–8].

Owing to the versatile properties of hydrochars and their economic viability, they have gained increasing importance and have replaced AC-based applications, such as capacitors [9], energy storage [10], soil amelioration, and adsorbents for water purification [11]. ACs are generally prepared by physical and chemical activation processes. Both processes require pyrolysis and additional activation steps by gases or chemical agents that result in energy and economic compromise. Being a cheap and efficient alternative, hydrochars, particularly their application to pollutant removal, have been the center of many scientific research interests. However, studies performed with ACs have shown that carbon adsorbents with a lower content of oxygen functional groups, would present a higher sorption capacity for removal of organics when compared with carbon adsorbents with high contents of oxygen functional groups. Due to low ash contents, hydrochars serve the best precursors in preparation of AC. Hydrochars based activated carbons from orange peels have been tested for the treatment of certain emerging pharmaceutical pollutants. Activation process, surface texture, and pH reportedly exert a significant influence on adsorption features [5]. Some anionic dyes have also been investigated in terms of the removal efficiency of food waste-based hydrochars with an advanced approach in which an artificial neural network design is developed for an automated wastewater treatment plant [12]. Surface modified hydrochars have also been investigated for metal removal [4]. Meanwhile, hydrochars outperform ACs in certain applications, but no review article has focused on the applications of lignocellulose based hydrochars and activated carbons derived from them to the adsorption of ECs and EDCs. Dai et al. [13,14] reviewed the application of agriculture wastes and biochars to the removal of different contaminants and organic contaminants, respectively. Bhatnagar and Anastopoulus [15] summarized the different types of adsorbents for bisphenol A removal, and Kim et al. [16] reviewed the use of graphene-based adsorbents for various organic and inorganic contaminants. Therefore, the present review focuses on and discusses the recent advances in hydrochar and activated carbon formation, their applications in removing ECs and EDCs, and the gaps associated with the adsorption performance of hydrochars and activated carbons derived from them. Recommendations for the future improvement of these materials are also detailed from economic and applied industrial perspectives.

2. Classification and sources of ECs

ECs are new and known toxic pollutants that belong to different classes, such as pharmaceuticals containing nonsteroidal anti-inflammatory drugs, antibiotics and antifungal/antimicrobial agents, fragrances, pesticides, food additives, artificial sweeteners, lipid regulators, hormones, UV filters, flame retardants, and other industrial products [17,18]. Despite these classifications, confusion remains in categorizing different pollutants. For example, some plasticizers that are considered endocrine disrupting compounds are also called ECs. This ambiguity indicates that ECs are a broad spectrum of pollutants that pose hazardous impacts on humans and aquatic organisms in all aspects [17]. Fig. 1 shows the classification of ECs, which are chiefly found in many commercial and household products, according to the literature [19].

The common sources and pathways of ECs that lead to contamination in the environment include wastewaters from local wastewater treatment units [20], hospitals [21], livestock activities [22], food processing plants, agriculture waste, subsurface storage of industrial and household wastes, and indirect means of ground water surface

Fig. 1. ECs pollutants.

water exchange [23]. Generally, ECs can be introduced to environment from two main sources, namely, point and diffuse sources. First sources are identified or specific sites of pollutants, and the input can be identified in a spatially separated way. Examples of such sources include different industrial effluents, cosmetics, hospitals, sewage treatment plants, mining activities, buried septic tanks, and waste lagoons. The discharge of contaminants from these sources is usually concentrated. Meanwhile, diffuse sources refer to unidentified or indistinct sources. Examples include run-offs from biosolids or manure and floods in industrial or urban regions. The discharge from these sources is often low and cannot be controlled. Fig. 2 schematically explains the different sources from which ECs are discharged and enter the surface and ground waters. Surface water is more frequently loaded with ECs than groundwater is [24]. The animal, domestic, hospital and industrial wastes along with landfill represent the major source relative to a minor aerial source of ECs in surface and ground waters. Moreover, among these sources both landfill and aerial are the minor ECs pathways. The disposal from the households are considered important point sources as most of the unused or expired drugs are disposed through household solid waste or flushed down in the toilet. Artificial recharge/infiltration, with treated waste water from industrial and domestic or urban and stormwater runoff may become important basis of re-introducing these contaminants that might be still present in these waters. Animal feeding operations also present a major source of ECs as the significant portion of given antibiotics, pesticides or hormones passes through the livestock and is excreted and stored in waste lagoons.

3. Classification and sources of EDCs

EDCs are exogenous agents that alter the natural functions of the hormones in our body that are responsible for homeostasis, development, and reproduction [25]. According to the review by Tijani et al. [26], nearly 38,000 different chemicals and elements have been identified as EDCs. These are classified to synthetic and natural hormones such as estrone, 17 β estradiol (E2), estriol testosterone, dihydrotestosterone [27]; ethynylestradiol and phytoestrogens [28]; industrial compounds such as bisphenol A, phthalates, parabens, nonylphenol, and perfluorooctanesulfonate [29,30]; dioxins; flame retardants, including polybrominated diphenyl ethers; various medicines such as diethylstilbestrol; pesticides such as endosulfan and

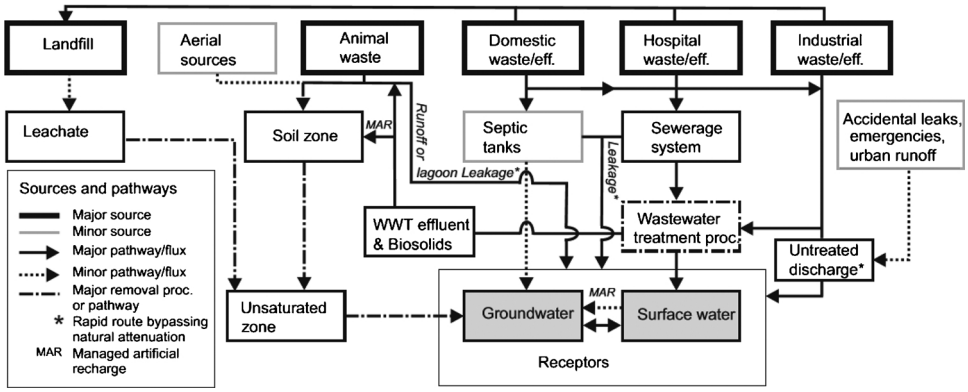

Fig. 2. Schematic presentation of sources and pathways of ECs discharged into the environment [24].

organophosphorus pesticides; and synthetic birth control pills [28].

EDCs are also considered ECs due to their uncertain prolonged health impacts. The sources of EDCs are widespread and diverse in nature. Similar to ECs, EDCs are commonly found in low concentrations (ng-μg/L level) in sewage wastewater treatment plants, surface water, ground water, hospital wastewater, soil, sediments, air, and even drinking water [31–35]. Mostly industrial effluents after being treated are directly introduced to the ground water where traces of EDCs still remain and thereby enter to the aqueous environment. Some pesticides in agriculture applications directly absorb into soil and may leach to the ground water and then make their way to the food chain by building up in fish, animals and humans. According to the recent research of Saeed et al. [36], significant concentrations of phthalates, alkyl phenols, and estrogens have been detected in coastal areas receiving sewage discharge. Different alarming concentrations of phthalates have also been found in the sediments of the northern part of the Arabian Gulf, and they may have entered via industrial and agricultural activities [37]. This finding suggests that EDCs prevail heavily in water and airborne dust particles. Therefore, strict guidelines and protocols must be implemented to restrain the discharge of these toxic and hazardous pollutants from their sources.

4. Lignocellulosic biomass

In terms of renewability, recyclability, and sustainability, biomass-based resources are a main concern from the economic and energy perspectives. Lignocellulosic biomass is a non-edible and renewable resource in different industrial applications, such as production of biofuels (i.e., bioethanol, biobutanol, and biomethanol), value-added chemicals, and new polymers [38–40]. Lignocellulose biomass forms a significant fraction of forestry and agricultural crop wastes. Decreasing sources of fossils, increasing economic demands, and environmental pollution from greenhouse gases have urged today's scientific community to utilize lignocellulose biomass as an alternate renewable source. In the context of agricultural and environmental restraints, biomass resources are expected to supply power of 130–270 EJ/year in 2050. This value can satisfy 15 %–25 % of the future total energy requirement [41]. Lignocellulose biomass mainly consists of three main structural components, namely, hemicellulose (20–40 %), cellulose (40 %–60 %), and lignin (10–25 %) [42]. Depending on a wide variety of sources, these materials may be processed to achieve different industrially important chemicals and biofuels for internal combustion engines. Given the recalcitrance of the lignocellulose network, these materials undergo different modes of pretreatment, such as hydrothermal methods (including steam and CO_2 explosions), hot water treatment, chemical methods (involving acid and base treatments), organosolv methods using organic solvents, ammonia recycle percolation, ammonia fiber explosion, and ozonolysis [40], to destroy their structures and achieve different fermentable sugars for obtaining alcohols and other value-added products [38,43].

The adsorption performance of lignocellulose biomass may be improved via substantial treatments, such as chemical, physical, physico-chemical, and thermochemical treatments. These treatments may introduce novel functionalities that are compatible with target pollutants. Among the numerous treatment protocols, HTC is considered as an eco-friendly and cost-effective technique and is further discussed in the next section.

5. Hydrothermal carbonization

Hydrothermal carbonization or wet torrefaction is a thermo-chemical method of converting biomass of low heating value and large moisture content into carbonaceous solid residues with chemical characteristics identical to those of lignite coal, surrounding liquids (e.g., furfurals and small organic acids, including acetic, lactic, and levulinic acids), and gaseous by-products [44,45]. The aqueous suspension of biomass is treated at the subcritical temperature of approximately 180 °C – 250 °C in a closed reactor under autogenous pressure. The solid residue from the hydrothermal treatment is called hydrochar by the European Biomass Industry Association [46]. HTC is considered a simple and easily scalable technology that is suitable for any organic raw biomass.

In addition to its valorization, HTC is made advantageous by its use of water as a reaction medium and catalyst that is nontoxic, cheap, and ecofriendly; under a subcritical temperature, the characteristic features of water dramatically change, the hydrogen bonds weaken, the dielectric constants decrease, and the ionization of water begins as the number of hydronium ions (H_3O^+) increase to facilitate the hydrolysis of glycosidic linkages in the hemicelluloses in biomass into hexoses and pentoses for subsequent transformation into value-added chemicals [47]. Moreover, this technique is applicable to biomasses with high moisture contents (60 % humidity) and is different from pyrolysis, which is unsuitable for biomasses with high moisture contents and those that require sufficient pre-drying before being properly utilized. Such treatment may enhance the consumption of energy. Moreover, toxic heavy metals are concentrated in chars after pyrolysis due to their thermal stability. By contrast, in HTC treatment, these heavy metal contents are sufficiently removed from hydrochars through transformation into the liquid phase, which leaves stable carbonized fractions [48,49].

5.1. Hydrothermal carbonization of lignocellulosic biomass to hydrochar

The hydrothermal carbonization process is generally affected by operation temperature and residence time. The properties of resulting hydrochars depend not only on these factors but also on the nature and composition of feedstock. Table 1 summarizes the yields and characteristics of hydrochars and their lignocellulose feedstocks [50–55].

Table 1
Mass yields and the characteristics of hydrochars and their lignocellulose biomass feedstocks.

Lignocellulose biomass or its hydrochar (HC)	Mass Yield (%)	C (%)	H (%)	O (%)	Other elements (%)	Ash (%)	HHV (MJ/kg)	References
Wood-HC	60.3 %	52.4	5.8	48.8	–	–	–	[50]
Wood		48.1	5.6	46.3	–	–	–	
Corn stalk-HC	56.92	49.23	5.94	36.35	N 1.16, S 0.17	7.15	19.66	[51]
Corn stalk		43.11	5.73	42.4	N 0.92, S 0.31	7.12	17.19	
Corn stalk digestate-HC	62.20	42.65	4.50	29.22	N 1.53, S 0.35	21.75	17.16	[51]
Corn stalk digestate		38.01	4.79	38.33	N 2.05, S 0.62	16.2	15.86	
Wheat straw-HC	49.2	60.6	5.57	29.5	N 0.58, S 0.40	3.26	23.8	[52]
Wheat straw		45.03	5.70	44.56	N 0.44, S 0.37	3.90	17.60	
Willow-HC	40	70.4	5.3	20.2	N 1.30, S 0.10	2.7	27.8	[53]
Willow		45.3	6.2	43.8	N 0.50, S 0.10	4.10	16.40	
Miscanthus-HC	45	71	7.9	17.5	N 1.1, S 0.20	2.3	32.1	[53]
Miscanthus		46.0	5.7	42.8	N 0.5, S 0.1	4.9	16.1	
Oak wood-HC	43	72.2	6.6	15.2	N 2.2, S 0.2	3.6	31.1	[53]
Oak wood		43.4	5.9	42.9	N 0.3, S 0.1	7.40	15.40	
Greenhouse waste-HC	45	68.5	6.1	17.4	N 3.6, S 0.2	4.2	28.8	[53]
Greenhouse waste		45.7	6.7	36.4	N 1.1, S 0.2	9.9	18.5	
Acacia-HC	70	59	5.85	34.5	N 0.18, S 0.0	0.47	21.5	[54]
Acacia		47.0	5.76	46.96	N 0.11, S 0.01	0.16	–	
Pine-HC	79	62.7	6.49	30.5	N 0.06, S 0.0	0.2	23.8	[54]
Pine		48.10	6.57	45.12	N 0.10, S 0.01	0.10	–	
Corn silage-HC	52.5	64.4	5.4	26.9	N 1.60	–	26.6	[55]
Corn silage		46.9	6.20	41.9	N 1.2	–	19.60	

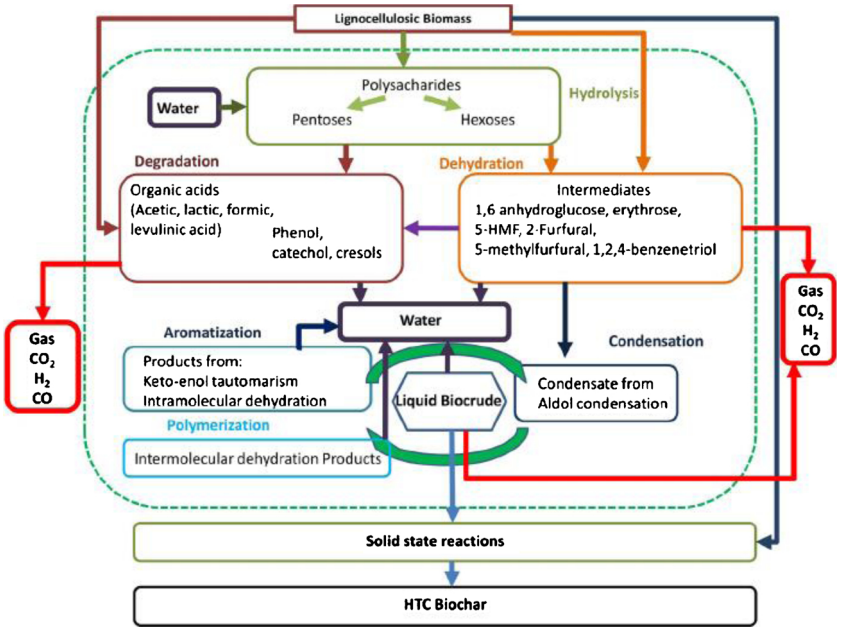

Fig. 3. HTC reaction pathways from lignocellulose biomass [8].

The degree of carbonization is determined by H/C and O/C ratios. Decreasing ratios of these elements suggest increased carbonization values, whereas O/C values suggest the presence of oxygenated functional groups (OFGs) [56]. During HTC, the hemicellulose part of the lignocellulose biomass is prone to degradation due to the low activation energy and is converted to volatile products [54]. However, cellulose and lignin are resistant to degradation below 220 °C. The thermal stability of these species follows the order: lignin < cellulose < hemicellulose [57]. The HTC of lignocellulose biomass involves different steps of reactions that occur simultaneously, such as hydrolysis, dehydration, decarboxylation, aromatization, condensation, and polymerization [58]. With an increase in temperature, the ionic product of water is believed to increase, making water a weak acid/base catalyst. Consequently, a hydrolysis reaction commences with the breakage of the ether bonds in hemicellulose and cellulose; in this case, lignin is mostly unaffected. The resulting monomers and oligomers then move toward the aqueous phase and are further degraded into various small chemicals (Fig. 3). This process leaves small pores on the solid residue.

Hydrochar properties are also greatly influenced by feed water pH. Hydrochars were produced from wheat straw by changing the acidic and basic pH of feed water. Hydrochars with great pore properties were derived using the acidic pH of feed water. Furthermore, the production of sugars, furfurals, and organic acids under basic pH was found to be low [59]. The metal retention in the form of ash is also a crucial factor, that is, the ash contents in hydrochars mostly decrease relative to their raw materials. The ash contents further decrease with reaction severity. High ash contents in hydrochars may impair the application of the latter as solid fuel and may cause slagging and fouling during combustion. The presence of inorganic species, such as Na, K, Ca, Mg, P, and N, greatly affects the formation features of hydrochars [53]. However, a knowledge gap exists with regard to the role of these elements in the hydrochar formation mechanism and their effects on the composition, production, and characteristics of hydrochars.

Lignocellulose biomass as feedstock has many benefits, such as

abundance and low cost. When mixed with other non-lignocellulose biomasses, this raw feedstock can be applied as high-quality solid fuel [60] and as an excellent material for soil amelioration [61], and it can reduce heavy metal content relative to individual feedstocks [62]. Microwave-integrated HTC is currently considered appealing as it accelerates hydrochar formation, but this technique is underutilized due to its lower yields in comparison with those of conventional thermal methods, the difficulty in processing tons of biomasses, and its energy intensiveness [58,63]. Microwave-produced hydrochars have been reported to serve as an alternative to raw coal that could reduce the cost to half when used as an energy source [64].

The pore properties and yield of hydrochars significantly depend on the composition of lignocellulose feedstocks in terms of hemicellulose, cellulose, and lignin. Moreover, HTC temperature and acidic pH of feed water play a role in enhancement of pore properties of hydrochars. From Table 1, the high carbon and oxygen contents along with the low ash content of lignocellulose feedstocks result in the formation of hydrochars with large yield (40–79 %) and favorable heating value (17.16–32.1 MJ/kg) and carbon content (42.65–72.2 %). In addition, the low nitrogen and sulfur contents of these feedstocks produce hydrochars with less nitrogen (0.06–3.6 %) and sulfur (0.1 − 0.46%) elements. Thus, lignocellulose feedstocks derived hydrochar can be efficient and eco-friendly precursor for ACs with low emission of noxious gases during activation.

5.2. Preparation of ACs from lignocellulosic biomass by conjunction HTC and subsequent activation

Generally, the AC requirement increases annually by approximately 8.1 % and may reach up to 2.1 million metric tons in the coming years; this change may further increase the AC cost [65]. Therefore, many researchers are now switching to cheap and renewable lignocellulose biomasses as carbon sources. ACs are normally prepared by the carbonization of precursors at the temperature range of 600 °C – 700 °C (dry method) for a certain time. In the traditional process, which is still used today, the smoke from the process is freely emitted to the atmosphere, thus contributing to environmental pollution, and most of the ash is deposited on the resulting carbon. These results call for an energy-efficient separation process for obtaining pure AC. As part of the effort to save energy and cut down the cost of AC production, HTC (wet process) is used to produce hydrochars before their activation to AC. Normally, HTC is conducted at 180 °C – 250 °C, which is much lower than that in the carbonization process. Moreover, HTC does not emit smoke to the atmosphere and produces minimal ash in the resulting hydrochars. Moreover, the use of water in HTC could produce hydrochars with many new functional groups (OH, −COOH, −CHO) on the surface that can enhance adsorption capacity. Using HTC-based hydrochars as a carbon source could offer many benefits: (i) provide an economic, ecofriendly, and sustainable way of reutilizing waste biomass; (ii) yield a purified carbon source with abundant OFGs that facilitate activation to generate ACs with a large surface area; and (iii) create efficient and cheap adsorbent or catalyst support/raw materials that could efficiently replace commercially available ACs. Table 2 shows the textural properties of some ACs produced through the activation of hydrothermally treated lignocellulose biomasses [66–75].

Generally, the formation of ACs with superior porosities and surface areas is promoted by the use of suitable activation agents at optimum proportion and suitable operation temperatures at a certain time. Activation agents, such as KOH, NaOH, $ZnCl_2$, and H_3PO_4, have been widely studied to produce porous ACs.

Acid activators are preferred to alkali metal hydroxides as they remove inorganic impurities and can be easily recovered from the process [76]. In addition, acid treatment can introduce abundant oxygen containing functional groups to the resulting hydrochar [77]. Rice husk-based hydrochars were chemically treated with H_3PO_4, and AC with a BET surface area of 2700 m^2/g was obtained at 500 °C for capacitor application [68]. Activation with H_3PO_4 is considered to occur under mild conditions; the case is different for ACs obtained by alkali activation. In this context, both rattan stalks and coconut shell-derived hydrochars were chemically activated with NaOH at 600 °C to produce ACs with BET surface areas of 1135 and 876.14 m^2/g, respectively [70,71]. NaOH activation resulted in a mesoporous structure and uniform surface (Fig. 4). The development of ACs porosity is attributed to activator's dehydration effect, which breaks the C—O—C and C—C bonds of hydrochar. NaOH is reduced to metallic sodium Na, hydrogen gas, and sodium carbonate Na_2CO_3. Furthermore, Na_2CO_3 is degraded into Na and CO as follows [78]:

$$6\ NaOH + 2\ C \rightarrow 2\ Na + 3\ H_2 + 2\ Na_2CO_3 \quad (1)$$

$$Na_2CO_3 + 2C \rightarrow 2Na + 3CO \quad (2)$$

Thus, both the alkaline and carbonate metals are intercalated into the hydrochar structure and played a role in generation and enlargement of pores. Few studies have reported the use of K_2CO_3 as an activator because it is known to be non-deleterious unlike KOH. Magnetic ACs have been prepared from *Salix psammophila* and rice straw hydrochars using K_2CO_3 as the activator with a 2:1 impregnation ratio. The resulting product performs well in the adsorption application due to its excellent surface area with microporous and mesoporous structures, respectively [69,73].

Hydrochars may serve as ideal precursors for preparing ACs for multiple applications because they evidently reduce energy consumption and environmental concerns. According to Table 2, hydrochars derived ACs exhibit high surface areas within the range of 876 to 2960 m^2/g. Different basic, acidic, and metallic salt activators are applied for the production of ACs with well-developed pores and microporous or mesoporous structures depending on the type of activator and activation conditions. Despite increasing research work, gaps remain in current technology, and some of them are mentioned here. Suitable activating agents should not only be cost-effective but also environmentally benign and easily recoverable. No work has explored the use of value-added acids, like lactic acids, levulinic acid, and acetic acid produced from the HTL of biomass for the activation of resulting

Table 2
Textural characteristics of AC derived from lignocellulose-based hydrochars.

Lignocellulose biomass	Activating agent	HTC Temperature °C	Activation Temperature °C	Pore Volume cm^3/g	Surface Area m^2/g	References
Eucalyptus sawdust	$K_2C_2O_4$ and melamine (1/6/2)	250	800	1.6	2960	[66]
Eucalyptus sawdust	KOH (1/4)	250	700	1.03	2252	[67]
Rice husk	H_3PO_4 (1/2.5)	95	500	~1.6	2700	[68]
Rice straw	K_2CO_3 (1:2)	300	800	1.07	1334	[69]
Rattan (Lacosperma secundiflorum)	NaOH (1:3)	200	600	0.6	1135	[70]
Coconut shell	NaOH	200	600	0.44	876.14	[71]
Date seeds	NaOH (1:3)	200	600	0.66	1282	[72]
Salix psammophila	K_2CO_3 (1:2)	–	800	0.943	1541	[73]
Coconut shell	$ZnCl_2$ (1:3)	200	800	1.5	2050	[74]
Coconut shell	$ZnCl_2$ (1:2)	275	800	1.17	1673	[75]

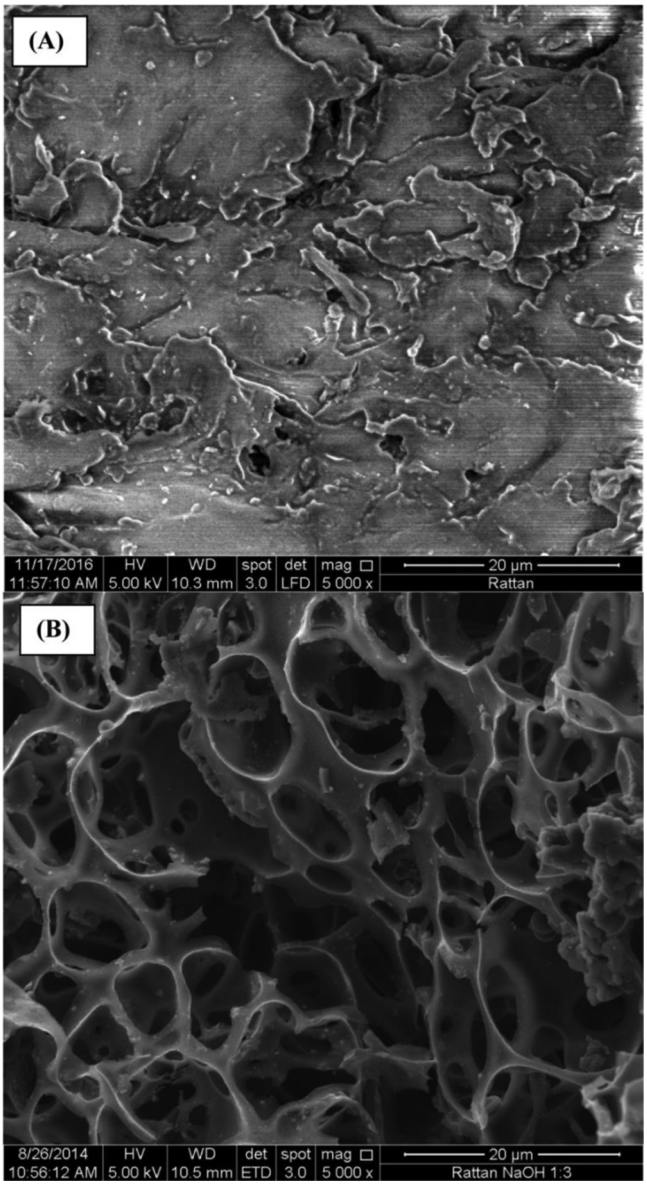

Fig. 4. SEM images of (A) raw rattan and (B) rattan-based AC [70].

hydrochars. Using such biomass-derived activating agents may exert some profound effects on AC production yield and textural properties and may reduce the cost of the method. New strategies should be developed to overcome high temperature requirements and low AC yields. In this regard, few catalysts may be developed, or equipment design should be engineered. Few new applications of hydrochar-based carbons, such as fuel cells, membrane materials for ECs, and EDC removal from wastewater treatment plants, should also be explored to offer sufficient removal below permissible limits. Large-scale production, cost estimation, and the stability of hydrochars should be considered from an industrial point of view.

6. Mechanism of adsorption of ECs and EDCs on hydrochar and ACs

The mechanism of adsorption involves a combination of a multitude of interactions, i.e. hydrogen bonding, pore filling, hydrophobic interactions, and π-π interactions. This combination depends on different factors, such as surface chemistry, surface area, pore size, surface charge (zeta potential), pH, and the chemical structure of target compounds. All these interactions occur either simultaneously or by changing the experimental parameters, especially pH. Surface texture and functional groups greatly affect the adsorption mechanism. Although suggesting the exact mechanism taking place is difficult, many researchers favor Fourier-transform infrared spectroscopy (FTIR) as a useful tool to investigate the interactions between solutes and adsorbents. Relying on FTIR and surface charge results may arbitrarily predict the mechanism; however, we feel that the assistance of further advanced surface techniques is crucial in investigating the exact mechanism because mechanisms are essentially complex and require careful investigation. Table 3 shows different predominant adsorption mechanisms that are responsible for the effective removal of ECs and EDCs by hydrochars or the ACs derived from them [79–92].

Solution pH has a pivotal role in tuning the surface charges and active functional groups of target analytes. It can alter the adsorption mechanism from being hydrophobic to being electrostatic. A change in pH induces positive/negative charges on hydrochars/AC and the molecular state of solute and thereby affects electrostatic interactions. The structure of hydrochars involves a hydrophilic shell, which results from abundant OFGs; and a hydrophobic core, which results from fixed carbon and aromatization [79]. Kyzas and Deliyanni [88] suggested that ACs from potato peel hydrochars, when subjected to HNO_3 oxidation, produce an enhanced number of OFGs for the adsorption of pramipexole dihydrochloride and dorzolamide. FTIR spectrum results confirmed the presence of O—H group of the phenol at 3400 cm^{-1} and C—C group of the aromatic ring at 1615 cm^{-1}. After the adsorption, the disappearing of O—H group and shifting of C—C group was observed which indicated the role of these groups in adsorption process. Thus, the mechanism is mainly π-π electron coupling and Lewis acid–base reactions between amino groups in drugs and O in AC. Furthermore, pH exerts a strong influence on uptake behavior because acidic pH 2 provides the highest removal efficiency that declines with a further rise in pH due to electrostatic repulsions. A highly basic pH is unfavorable for most pollutants, such as E2 that is removed by Fe–Mn binary oxide-functionalized hydrochar (PZC ~ 5) as E2 remains in neutral state at pH < 10. FTIR spectrum showed the peaks at 3415 cm^{-1} and 1508 cm^{-1} which attributed to the O—H and aromatic C—C stretching bonds, respectively. Owing to the aromatic structure and presence of OH groups, the principal adsorption mechanism was proposed to be π-π interactions and hydrogen bonding [80]. A similar observation was also found by Li et al. [87], who tested the adsorption of amoxicillin onto AC from previously modified hydrochars from corn stalks. The presence of amoxicillin in different chemical forms at different pH levels and zeta potentials of the adsorbent affected the adsorption mechanism. The removal of salicylic acid and flurbiprofen on AC from orange peel hydrochar was also found to be pH-dependent, with the acidic pH being the most suitable for maximum removal. Here, dispersion was the main interaction proposed, along with a slight electrostatic interaction between positively charged adsorbents and π electron of drug molecules. FTIR results only displayed a single peak at 1612 cm^{-1} that accounted for the complete disappearance of carboxylic groups and the presence of aromatic C—C group, indicating that only hard carbon components remained [5].

In some cases, changes in pH do not affect adsorption behavior; for example, Chen et al. [86] observed that changes in pH had no effect on the adsorption of tetracycline using magnetic AC derived from fir saw dust hydrochar. In another study, the removal of E2 and 17α-ethynylestradiol by montmorillonite/hydrochar composites was relatively the same within wide pH ranges due to stable hydrogen bonds, π-π interactions, and intercalation [81]. Suo et al. [92] also found no significant effect of pH on organophosphorus pesticides removed by AC from corn straw cellulose and graphene composites because the main mechanism was preferentially π-π interactions.

In a Raman study, the degree of graphitization (I_D/I_G) was expected to play a vital role; that is, increasing activation temperatures lead to burn out that causes extensive dislocations and defects, which in turn improve the surface area and adsorption properties of the resulting

Table 3
Types of adsorption mechanisms of ECs and EDCs on hydrochars and ACs from hydrochars obtained from different lignocellulose biomasses.

Lignocellulose biomass	Pollutant	Category	Optimum pH	Amount of adsorbent (g or mg)	Temperature (K or °C)	Mechanism responsible for adsorption	Reference-s
Hydrochars							
Argun Nut shells	Bisphenol A	EC as well as EDC	6.5	0.01 g	293 K	• π-π interactions • Hydrogen bonding. • Pore filling	[79]
Argun Nut shells	Diuron	EDC	6.7	0.01 g	293 K	• π-π interactions • Hydrogen bonding. • Pore filling	[79]
Rice husk hydrochar with Fe-Mn binary oxides	17β-estradiol	EDC	7	5 mg	28°C	• π-π interactions • Hydrogen bonding	[80]
Montmorillonite/Hydrochars from rice husk	17β-estradiol and 17α-ethinylestradiol	EDC	7	5 mg	25°C	• π-π interactions • Hydrogen bonding • Intercalation between clay layers • Electrostatic interactions	[81]
Rice husks	Herbicide: octhilinone(2-octyl-4-isothiazolin-3-one) Antibiotics:trimethoprim, sulfamethoxasole, and ciprofloxacin Pharmaceuticals (diclofenac, paracetamol, diphenhydramine, and fluconazole)	EC	–	50 mg	20°C	• Hydrophobic interactions (based upon higher $logK_{OW}$) • Hydrogen bonding	[82]
Rice husks	Triclosan bisphenol A	EDC as well as EC	–	50 mg	20°C	• Hydrophobic interactions (based upon higher $logK_{OW}$) • Hydrogen bonding	[82]
Pistachio shells	Caffeine	EC	–	0.01 g	25°C	• Microporous diffusion • Interaction with surface and pore OH groups	[83]
Corn digestate, miscanthus and wood chips	Isoproturon	EC	–	195 t/ha	20°C	• Hydrogen bonding	[84]
Sulfamic acid modified saw dust hydrochar	Benzotriazole	EC	4 – 8	0.5 mg/L	–	• Electrostatic and nonelectrostatic • Complexing bridging interactions	[85]
Activated carbon from Hydrochars							
Fir saw dust with subsequent magnetization	Tetracycline	EC	5 – 9	20 mg	25°C	• π – π electron donor – acceptor interaction • Hydrogen bonding • Large surface area	[86]
Activated carbon from fore-modified cornstalks hydrochar	Amoxicillin	EC	7	1 g/L	20°C	• Electrostatic	[87]
Potato Peels Hydrochar followed by oxidation with HNO_3	Pramipexole and Dorzolamide	EC	2	0.02g	25°C	• π – π electron coupling • Lewis acid base interactions	[88]
Magnetic carbon from sugar cane bagasse based hydrochars	Tetracycline	EC	6.8	0.05 g	30°C	• Hydrogen bonding • π – π electron donor acceptor	[89]
Orange peel hydrochar	Diclofena, Salicylic acid, Flurbiprofen	EC	7 (Diclofenac), 2 (Salicylic acid and Flurbiprofen)	0.5 g/L	25°C	• Dispersive interactions and surface greater surface area (Diclofenac) • Dispersive and electrostatic (Both Salicylic acid and Flurbiprofen)	[5]
Magnetic hydrochars from Salix psammophila	Triclosan	EDC	–	0.5 g/L	30°C	• Pore filling	[95]
Hydrochar from green wastes	Atrazine	EC	–	2 mg	20°C	• Pore filling	[90]
Agave Americana fibers and mimosa tannin	Tetracycline		7	0.05 g	25 °C	• Pore diffusion	[91]
Rice straw derived hydrochar	Triclosan	EDC	–	50 mg/L	298K	• Porosity and surface area	[69]

carbon [86,92]. Zhu et al. [93] also observed that magnetic AC from sawdust hydrochars with great I_D/I_G possessed great porosities and great adsorption capability toward roxarsone (4-hydroxy-3-nitrophenylarsonic acid). The predominant adsorption mechanism was found to be pore filling, in addition to the mild surface complexation of As and Fe on the surface of the magnetic AC [93,94]. The same observation was found by Suo et al. [92] as discussed above. In another study by Zhu et al. [73], magnetic AC from *Salix psammophila* hydrochars was obtained at different temperatures. The sample was obtained at the lowest activation temperature and fixed hydrochar; the activator ratio had a great I_D/I_G ratio and the highest adsorption capacity toward triclosan.

Pore filling may be a dominant mechanism depending on the dimensions of the adsorbate. Fernandez et al. [5] found that the adsorption of salicylic acid is due to porosity development and that the molecular size of salicylic acid is smaller (0.6 nm) than the size of the pores on the AC from orange peel hydrochars. Zhu et al. [95] prepared magnetic AC from hydrochar at different temperatures for the removal of triclosan and obtained a linear increase in q_e values as functions of the surface area and pore and micropore volumes that led to the pore filling being the suitable mechanism. The removal of diuron and bisphenol A, in addition to hydrogen and π-π bonding, was explained by the presence of micropores [79]. The adsorption capacity of triclosan on AC from rice straw hydrochars was found to be several times greater than that of its magnetic derivative due to pore blockage by magnetic particles [69]. This result also suggested that the adsorption of triclosan was mainly based upon pore diffusion. FTIR spectrum displayed wide bands at 3400 and 1080 cm^{-1} which attributed to O—H and C—O groups. Being abundant in OFGs, hydrogen bonding interactions play a major role in adsorption with AC from rice straw hydrochars.

Sun et al. [96] compared the adsorption mechanisms of three EDCs, namely, bisphenol A, 17 ethynyl estradiol, and phenanthrene, on biochars and hydrochars. In addition to pore filling being the common mechanism, the adsorption of bisphenol A and 17 ethynyl estradiol was mainly due to hydrogen bonding, whereas phenanthrene was unable to facilitate hydrogen bonding due to the absence of OH groups but was able promote π-H bond and π-π interactions. In the study, the biochar showed mainly π-π interactions due to the existence of aromatic C═O, C—C, and C—H groups at 1700, 1600, and 885–752 cm^{-1}, respectively. In a special case, caffeine adsorption on AC derived from pistachio nut shell hydrochar was studied experimentally and by molecular modeling. The results based upon these two methods suggested that adsorption was mainly due to the microporous character of ACs. Prior to adsorption, caffeine formed aggregates that were disintegrated by surface OH groups on the adsorbent surface; with further disintegration, these molecules penetrated inside the pores and bound with the OH groups on the inner walls of the pores to make a monolayer attachment [83]. Fig. 5 illustrates adsorption mechanisms responsible for the adsorption of different EDCs and ECs by hydrochars and ACs derived from them [79,88,89].

Overall, many interaction mechanisms such as electrostatic, hydrogen bonding, pore filing, π-π interactions, and hydrophobic are proposed for EDCs and ECs adsorption on hydrochars and their derived ACs (Table 3). Solution pH, chemical structure of ECs or EDCs, and surface texture, functional groups, and surface charge of hydrochar or its derived AC greatly affect the adsorption mechanism. The mechanisms of adsorption of EDCs and ECs pollutants are mostly the same relative to other carbon-based materials obtained without hydrothermal treatment [97–99] but compared with hydrochars, AC derived from them offer enhanced adsorption capacities due to wider pore volumes and enhanced specific surface area [5,69,85]. Owing to the limited work on hydrochars or ACs derived from them for a limited number of ECs and EDCs, we need to employ new surface techniques to explore further the mechanisms of their adsorption and thereby understand the behavior of these pollutants. Correlation models should be developed to predict the influential interactions predominantly involved in the adsorption process. Weidemann

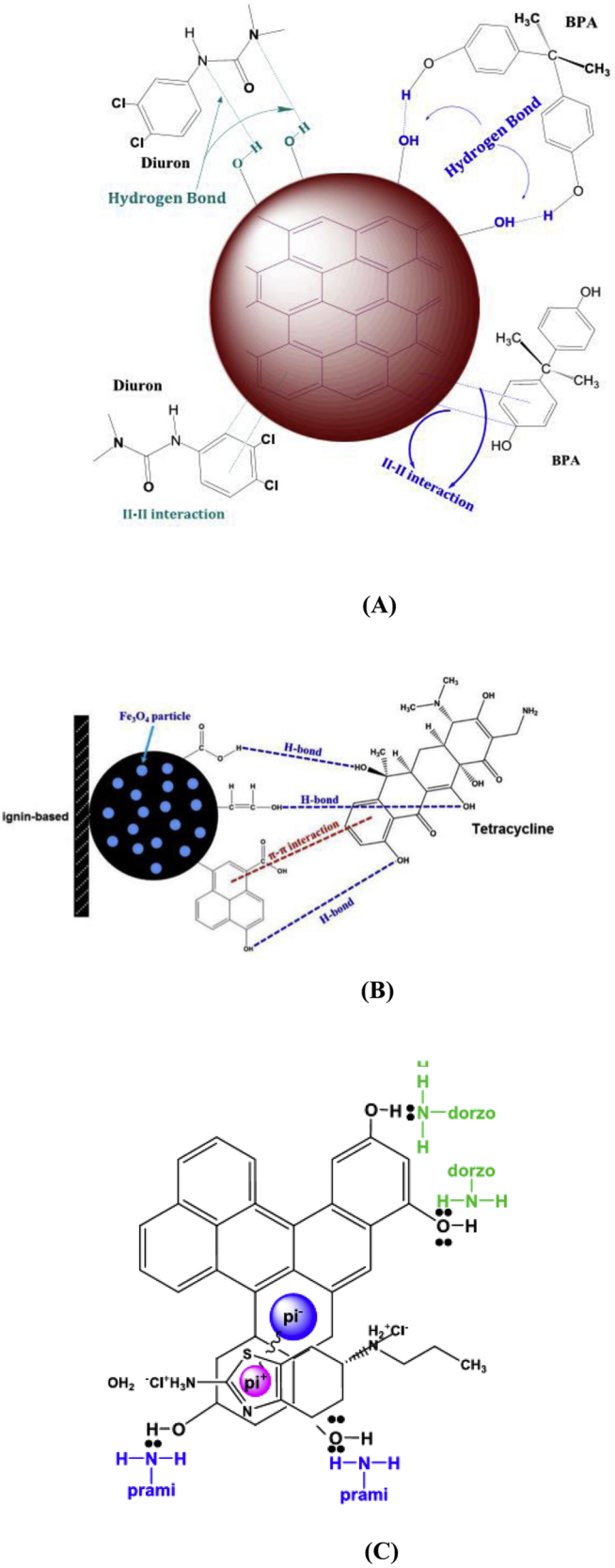

Fig. 5. Adsorption mechanisms from different hydrochars/ACs, (A) [79], (B) [89], (C) [88].

et al. [82] developed a correlation between the log K_{OW} values of fluconazole, ciprofloxacin, paracetamol, sulfamethoxazole, trimethoprim, ochthilinone, diphenhydramine, bisphenol A, diclofenac, and triclosan

and those of rice husk hydrochars, horse manure hydrochars, olive hydrochars, and tomato hydrochars. Among the hydrochars, those of rice husk had a positive correlation with the contaminants, thereby confirming hydrophobic interaction as the fundamental mechanism. The adsorption of additional EDCs and ECs, such as parabens, phthalates, and other industrial products, should be studied to widen the scope of lignocellulose-based hydrochars or ACs obtained by their post-treatment. Further work on real sample applications and their reusability is required.

7. Modeling of adsorption of ECs and EDCs on hydrochar and AC

7.1. Adsorption kinetic modeling

Both adsorption kinetics and equilibrium are baselines in designing and scaling up of adsorption systems. Kinetic studies involve modeling of experimental kinetic data collected by measuring the adsorbed amount against time. Pseudo-first- and pseudo-second order are the most generally applied empirical equations in liquid phase adsorption systems. Lagergren first proposed a pseudo-first-order equation with the following expression form [100]:

$$q_t = q_e - q_e e^{k_1 t} \tag{3}$$

Linearizing the above equation gives the following:

$$\ln(q_e - q_t) = \ln q_e - k_1 t \tag{4}$$

where q_e and q_t represent the adsorption capacities (mg/g) at equilibrium and time t (min) and k_1 is the rate parameter (1/min). An adsorption system is likely to follow this model under initial time intervals or prolonged intervals when the adsorption process is near equilibrium [101–103].

The pseudo-second-order equation suggests that the adsorption rate is second order function of available active sites and is used for large time intervals [104], whereas the pseudo-first-order equation is applied to describe adsorption at small time intervals. Mathematically, this model can be represented as

$$q_t = \frac{k_2 q_e^2 t}{1 + k_2 q_e t} \tag{5}$$

Linearizing the above equation gives the following form [104]:

$$\frac{t}{q_t} = \frac{1}{k_2 q_e^2} + \frac{t}{q_e} \tag{6}$$

where q_e and q_t denote the equilibrium adsorption capacities (mg/g) and adsorption capacities at a given time t (min) and k_2 is the rate parameter (g/mg/min). The adsorption kinetics of different pollutants frequently follow this model on the basis of high regression and low error analysis values and thereby signify this model's prominence. The fitted rate constants k_1 and k_2 are most probably lumped parameters that join reaction and diffusion influences under particular experimental variables; the determination of primary adsorption phenomena is scarcely discussed after model fitting [105]. Another model that predicts chemisorption is the Elovich equation [106], which is written as:

$$q_t = \frac{1}{\beta}(\ln \alpha\beta t) \tag{7}$$

Linearizing the above equation gives the following equation:

$$q_t = \frac{1}{\beta}\ln(\alpha\beta) + \frac{1}{\beta}\ln t \tag{8}$$

The plot between q_t and ln t should produce a straight line with $\frac{1}{\beta}$ slope and $\frac{\ln(\alpha\beta)}{\beta}$ intercept. α (mg/g/min) represents the rate constant, and β represents the extent of surface coverage and activation energy for chemisorption. Another commonly applied model is the Weber–Morris intraparticle diffusion model provided in the following equation [107]:

$$q_t = k_{id}\sqrt{t} + X \tag{9}$$

where k_{id} (mg/g. $\text{min}^{0.5}$) is the rate parameter and X is the initial adsorption (mg/g). For kinetics controlled solely by this model, a plot between q_t and $\sqrt{t}$ should be straight line passing through the origin (i.e., $X = 0$). Most research findings demonstrate multilinear curves within a studied time duration, and these curves are indicative of multiple mechanisms occurring simultaneously with controlling mechanisms, such as the transfer of solute to the external adsorbent surface, intraparticle diffusion, and the equilibrium stage, in which the solute adheres to the walls of the pores. These models are the most commonly studied and used to calculate rates and predict general adsorption mechanisms. The suitability of each model relies on the characteristics of the adsorbents, adsorbates, and experimental conditions.

Liu et al. [69] studied the removal of triclosan using AC and magnetic AC from rice straw-derived hydrochar. The experimental data were applied to validate different kinetic equations, like the pseudo-first-order, pseudo-second-order, intra-particle diffusion, and Elovich equations in linear mode. The results suggested the following order of best fittings: pseudo-second-order equation > pseudo-first-order equation > Elovich equation, according to the highest R^2 magnitudes and the small deviation between the experimental q_e and theoretical q_e values. The adsorption equilibrium was not immediately reached when high concentrations of triclosan were used. The rate k_2 of AC decreased (from 6.6×10^{-3} to 4×10^{-4} g/mg/min) with a rise in initial triclosan concentration, whereas the rate for the magnetic AC increased at high concentrations. The adsorption capacities of AC were higher (175–588 mg/g) than those of its magnetic derivatives (161–286 mg/g) due to the highly porous network. The application of the intraparticle diffusion model indicated a multilinear curve that produced a nonzero intercept, which reflected the rapid diffusion of triclosan on the external surfaces of the AC and magnetic AC, followed by diffusion inside the porous body. Kyzas and Deliyanni [88] developed oxidized AC from potato peel hydrochars and pyrolyzed potato peels for the removal of dorzolamide and pramipexole drugs. Linear plots of pseudo-second- and pseudo-first-order models revealed that the former can effectively explain adsorption kinetics. According to the closeness of the experimental q_e values to the calculated q_e values (PP-HYD-ox/prami: $q_{e,cal}$ = 31.3 mg/g and $q_{e,exp}$ = 31.1 mg/g), (PP-HYD-ox/dorzo: $q_{e,cal}$ = 30.5 mg/g and $q_{e,exp}$ = 30.4 mg/g) were greater than those of the AC obtained from pyrolyzed potato peels. The rate of adsorption using AC from pyrolyzed potato peels was greater than that using a hydrochar precursor; this result implied faster adsorption in the former than in the latter.

Given that the pseudo-second-order equation is preferentially more valid than other kinetic models are, most research groups only applied this model to determine the rates and adsorption capacities of adsorbents. Plazinski et al. [108] showed that the preferential fitting of the pseudo-second-order equation over the pseudo-first-order equation can stem from a theoretical basis rather than a physical one. The random errors in the calculated q_e values did not vary to a great extent during the linearization of the pseudo-second-order equation, as in the case of the pseudo-first-order equation. An additional benefit of using the pseudo-second-order equation is that equilibrium q_e is not required for data fitting. Zhu et al. [93] prepared hydrochars using different temperature ranges (i.e., 160 °C – 300 °C) for the hydrothermal treatment of sawdust from a furniture factory. The resultant samples were simultaneously activated and magnetized to obtain magnetic ACs. The samples were studied for the removal of roxarsone. The magnetic AC obtained from the hydrochars at 160 °C exhibited high pore properties. Applying the linear form of the pseudo-second-order equation showed that the adsorption rate was high, which suggested the excellent

adsorption of roxarsone on the as-prepared samples. The adsorption capacities (q_e = 515 mg/g) and rates of adsorption (13.2×10^{-4} g/mg/min) increased in the following order: MC-160 > MC-200 > MC-240 > MC-270 > MC-300. This order was mainly due to the favorable pore filling on the magnetic AC obtained from the hydrochars at low temperatures. Similarly, Chen et al. [86] applied the pseudo-second-order equation to the experimental data of tetracycline adsorption on AC and magnetic AC from saw dust hydrochars. The maximum adsorption capacities achieved were 250 mg/g using ACs and magnetic ACs, but the former achieved equilibrium earlier (10 min) than the latter did (30 min). On the basis of this model, the authors assumed the rate-limiting step to be chemisorption in nature. An increase in initial solute concentration tends to increase equilibrium time.

Fernandez et al. [5] prepared AC from orange peel hydrochars using air, CO_2, and phosphoric acid as activating agents for the removal of diclofenac, salicylic acid, and flurbiprofen, respectively. The kinetic data were as correlated to only the pseudo-second-order equation in nonlinear mode (Fig. 6). The adsorbed amount of diclofenac was high on acid-AC, whereas those of salicylic acid and flurbiprofen were high on air-AC. The rates of adsorption of diclofenac and flurbiprofen were high on H_3PO_4-treated AC from acid-treated hydrochar, whereas those of salicylic acid were high on air-AC. The data on the adsorption of triclosan on γ-Fe_2O_3 AC prepared from *Salix psammophila* hydrochars revealed a preference for the pseudo-second-order equation. In that study, the effects of activation conditions influenced the q_e values (170.9–787.4 mg/g), and such an increase was correlated with different textural characteristics, like BET surface area, volume and size of pores [95].

Mesopore size and large micropore volume are responsible for great diffusion and fast rates of adsorption, as reported by Mestre et al. [109], who showed three types of AC, namely, AC prepared from sucrose hydrochars using KOH and K_2CO_3 as activating agents and commercial AC for the removal of paracetamol and iopamidol. This model was again preferentially fitted when Zhu et al. [110] studied the adsorption of tetracycline on magnetic porous carbon obtained from *Salix psammophila* hydrochars. The order of fitting was as follows: pseudo-second-order equation > pseudo-first-order equation > Elovich equation.

In another study, the adsorption of bisphenol A and diuron on Argan nut shell hydrochars represented by the pseudo-second-order equation with excellent determination coefficients better than it did the pseudo-first-order equation. The increase in temperature reduced the q_e values (1094–664 mg/g for bisphenol A and 773–557 mg/g for diuron), and the rate constant values dramatically increased with a rise in temperature (0.002–0.025 g/mg/min for bisphenol A and 0.013–0.208 g/mg/min for diuron). This detailed analysis suggested that temperature can only accelerate the adsorption system in some cases and that it may not necessarily increase adsorption capacities. Furthermore, the intraparticle diffusion model suggested two phase reactions, namely, macropore diffusion and mesopore diffusion [79]. By contrast, Ahsan et al. [99] suggested the first linear stage to be mesopore and macropore diffusion and the second stage linear curve to be micropore diffusion in their study of the adsorption of bisphenol A, sulfamethoxazole, and tetracycline on sulfuric acid-treated sawdust. The preferential fitting of the pseudo-second-order equation on every adsorption case reveals that the mechanism of adsorption depends on the presence of sufficient sites on adsorbents regardless of the type, preparation method, or aqueous environment used. Shi et al. [97] achieved a preferential fitting of the pseudo-second-order equation in their study of the adsorption kinetics of ciprofloxacin on Fe_3O_4/C from sucrose by HTC. The controlling mechanism was chemisorption in nature with a maximum q_e of 38.6 mg/g and rate of 19.9 g/(mg.h).

Li et al. [87] fitted nonlinear kinetic equations, namely, pseudo-first-order, pseudo-second-order, and Elovich equations, to the adsorption data of amoxicillin on AC from previously modified corn stalk hydrochar. Among these three models, the Elovich equation was found to have the best fit. Moreover, chemical adsorption, fast adsorption, and slow desorption were suggested to be the most suitable rate controlling mechanisms. Ning et al. [80] applied the nonlinear pseudo-first-order, pseudo-second-order, intraparticle diffusion, and Elovich equations to study the adsorption of E2 on Fe–Mn binary oxide-loaded hydrochars. As anticipated, kinetics preferentially followed the pseudo-second-order equation (q_e 47.43 mg/g and k_2 4.79 g/mg/min) with the following order: pseudo-second-order model > Elovich equation > pseudo-first-order model. Error analysis results, including the root mean square errors and chi-square statistics, also supported the validation of the pseudo-second-order equation. The Morris–Weber plot was multilinear, thereby implying that intraparticle diffusion was not the only governing mechanism.

Rattanachueskul et al. [89] used the nonlinear form of the pseudo-second-order equation to analyze the adsorption behavior of tetracycline on magnetic AC from sugar cane bagasse and obtained high rate constant values ($k_2 = 7.52 \times 10^{-4}$ g/mg/min; q_e = 28.14 mg/g). The authors elucidated the reason on the basis of the hierarchical structure of composites with macropores that were responsible for rapid diffusion; meanwhile, two-phase linear curves of intraparticle diffusion indicated film and intraparticle diffusion as the rate-limiting steps. Tetracycline adsorption with AC from hydrochars of *Agave Americana* fibers and tannin was also studied by the application of the nonlinear modes of the pseudo-first-order and pseudo-second-order models [91].

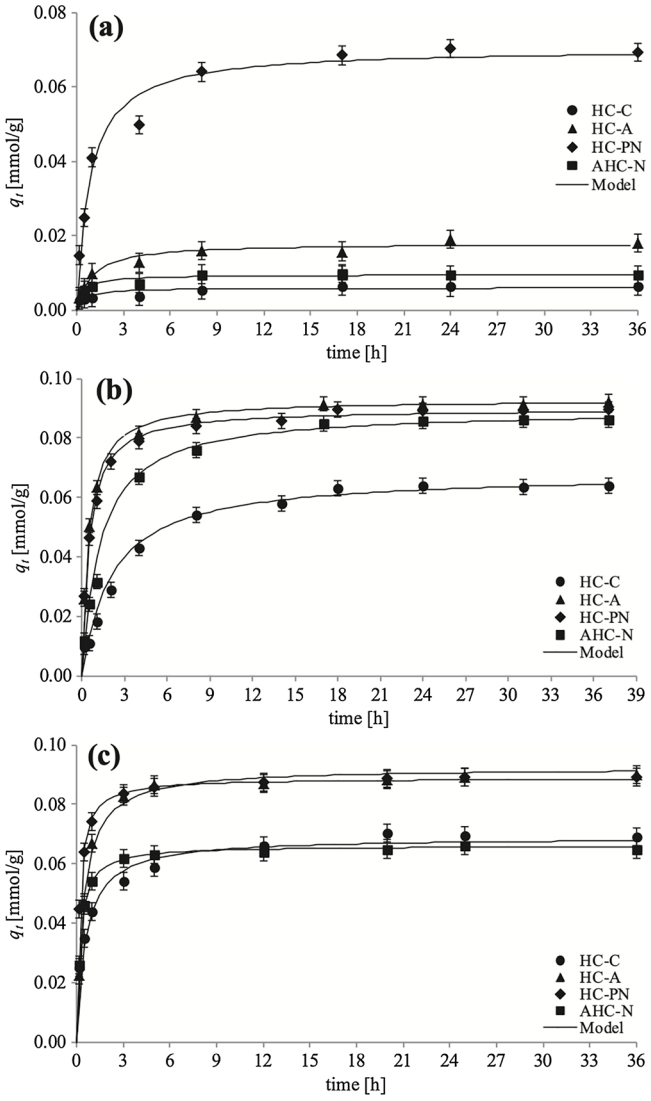

Fig. 6. Pseudo-second order kinetic for adsorption of (a) diclofenac sodium, (b) salicylic acid and (c) flurbiprofen onto the developed activated hydrochars [5].

Table 4
Kinetic models and parameters for the adsorption of different ECs and EDCs on lignocellulose-based hydrochars and their derived ACs.

Adsorbent	EC/EDC	Initial concentration and time range	Pseudo First order			Pseudo second order			Elovich Equation			References
			q_e (mg/g)	$k_{1\ (1/min)}$	R^2	q_e (mg/g)	k_2 g/mg/min	R^2	α (mg/g/min)	β (g/mg)	R^2	
Activated carbon from hydrochars of Agave Americana fibers in combination with tannin	Tetracycline	100 mg/L 0−400 min	45.24	0.038	0.919	49.79	0.0010	0.975	–	–	–	[91]
Hydrochars from Argun nut shells	Diuron	40 mg/L 0−180 min	5.24	0.031	0.141	775.1	0.013	0.99	–	–	–	[79]
Hydrochars from Argun nut shells	Bisphenol A	60 mg/L 0−180 min	5.24	0.010	0.115	1098.9	0.002	0.99	–	–	–	[79]
Montmorillonite rice husk hydrochar composites	17β estradiol	6 mg/L 0−24 h	103.3	0.7 (1/h)	0.856	113.8	0.0083	0.967	–	–	–	[81]
Montmorillonite rice husk hydrochar composites	17αethynyl estradiol	6 mg/L 0−24 h	65.77	2.25 1/h	0.842	68.8	2.21 g/mg/h	0.997	–	–	–	[81]
Magnetic activated carbon from sawdust hydrochars	Tetracycline	100 mg/L 0−120 min	–	–	–	250.5	0.0028	0.99	–	–	–	[86]
Fe-Mn binary oxide loaded hydrochars from rice husk	17 β-estradiol	6 mg/L 5 min to 48 h	42.2	0.013	0.877	47.43	4.79	0.971	4.68	0.14	0.95	[80]
Fore modified hydrchars from cornstalks	Amoxicillin	100 mg/L 0−90 min	88.8	3.77	0.992	89.97	0.124	0.997	1.65×10^{16}	2.07	0.992	[87]
Magnetic carbon composites from sugar cane bagasse hydrochar	Tetracycline	80 mg/L 0−26 h	–	–	–	48.35	7.52×10^{4}	–	–	–	–	[89]
Modified activated carbon from potato peel hydrochars	Pramipexole	50 mg/L 0−24 h	28.18	0.0153	0.976	31.3	9.6×10^{-4}	0.99	–	–	–	[88]
Modified activated carbon from potato peel hydrochars	Dorzolamide	50 mg/L 0−24 h	27.44	0.0142	0.941	30.5	9.3×10^{-4}	0.99	–	–	–	[88]
Magnetic activated carbon from sawdust	Roxarsone	400 mg/L 0−24 h	–	–	–	515.5	13.2×10^{-4}	0.99	–	–	–	[93]
Activated carbon from orange peel hydrochars through phosphoric acid activation	Diclofenac sodium	0.05 mM 0−36 h	–	–	–	0.07 mmol/g	16.6 g/mmol.h	0.97	–	–	–	[5]
Activated carbon from orange peel hydrochars through phosphoric acid activation	Salicylic acid	0.05 mM 0−36 h	–	–	–	0.09 mmol/g	23.6 g/mmol.h	0.993	–	–	–	[5]
Activated carbon from orange peel hydrochars through phosphoric acid activation	Flurbiprofen	0.05 mM 0−36 h	–	–	–	0.089 mmol/g	62.7 g/mmol.h	0.995	–	–	–	[5]
Activated carbon from rice straw-derived hydrochar	Triclosan	10 mg/L	8.94	0.014	0.52	175	0.0066	0.99	1.8×10^{16}	0.24	0.87	[69]
Magnetic Activated carbon from rice straw-derived hydrochar	Triclosan	10 mg/L	63.8	0.022	0.99	161	0.0010	0.99	4.6×10^{2}	0.05	0.95	[69]
γ-Fe_2O_3 carbon composite composites from hydrochars of Salix psammophila	Triclosan	50 mg/L 0−1400 min	–	–	–	763.4	1.1×10^{-4}	0.99	–	–	–	[95]

The pseudo-second-order model, as usual, had the best fit given its high determination coefficient (R^2) values and low error values. The experimental q_e 51.35 mg/g was close to the calculated one, and the rate constant was 2.48 g/(mg.min).

Furthermore, E2 and 17 α ethynyl estradiol followed the pseudo-second-order model with montmorillonite hydrochar composites activated by KOH [81]. The linear plots for E2 and 17 α-ethynyl estradiol yielded q_e = 113.8 mg/g and 68.8 mg/g, respectively. The rate constants for the adsorption of E2 and 17 α-ethynyl estradiol were 0.0083 and 2.21 g/mg/h, respectively. The mechanism was mainly proposed to be chemical in nature with the involvement of physical interactions.

The above discussion clearly reveals that the pseudo-second-order equation is the most frequently fitted model studied and that intraparticle diffusion is not the predominant rate-control step in all studies. All the above kinetic models were studied with different EDCs/ECs using hydrochars and their derived ACs and are summarized in Table 4.

7.2. Adsorption isotherm modeling

Generally, an adsorption isotherm is a curve that expresses the phenomenon that governs the retention of liquid/gas adsorbates on solid phase adsorbents by varying initial concentrations at particular temperature and pH [111]. Its physical parameters and underlying thermodynamic assumptions provide insights into the adsorption mechanism, surface properties, and degree of affinity of adsorbents. Two widely used empirical models, namely, the Langmuir and Freundlich isotherms, were adopted in different studies to determine the mechanism of adsorption and the maximum adsorption capacities. The Langmuir equation is given as [112]:

$$q_e = \frac{q_m b C_e}{1 + bC_e} \tag{9}$$

where q_e (mg/g) is the adsorbed amount at equilibrium, q_m (mg/g) is the highest adsorbed amount, and K_L (L/mg) is the Langmuir parameter.

The linearization of the above equation yields the following form:

$$\frac{C_e}{q_e} = \frac{1}{bq_m} + \frac{C_e}{q_m} \tag{10}$$

A dimensionless constant, also identified as the separation factor (R_L) suggested by Webber and Chakkravorti [113], can be expressed as:

$$R_L = \frac{1}{1 + K_L C_o} \tag{11}$$

where K_L corresponds to the Langmuir parameter and C_0 (mg/L) belongs to the initial adsorbate amount. The magnitude of this factor explains the nature of adsorption as unfavorable ($R_L > 1$), linear ($R_L = 1$), favorable ($0 < R_L < 1$), or irreversible ($R_L = 0$).

The Freundlich equation is expressed by the following [114]:

$$q_e = K_f C_e^{\frac{1}{n}} \tag{12}$$

The linearization of the above equation gives the following form:

$$\log q_e = \log K_f + \frac{1}{n} \log C_e \tag{13}$$

Here, K_f ((mg/g) (L/mg)$^{1/n}$) is the Freundlich parameter that represents adsorbed amount, and n is a parameter that indicates adsorption strength. The magnitude of $1/n$ between 0 and 1 is an index of adsorption strength or surface heterogeneity; as this value approaches 0, heterogeneity rises. Values below 1 imply chemisorption, and values above 1 indicate cooperative adsorption. The q_m values from the Langmuir isotherm are important in the selection of a suitable adsorbent and the design of an appropriate adsorption system. The Langmuir isotherm is a preliminary and simple model that retains unique importance, with almost every study determining adsorption capacity from this isotherm regardless of best fit because the value of q_m corresponds to the maximum monolayer adsorption capacity that other isotherm equations do not consider.

Table 5 shows two commonly applied empirical isotherm models and their parameters obtained from the adsorption data of different EDCs/ECs on different hydrochars or ACs derived from them. These isotherms greatly depend upon the nature of the adsorbent with different functional groups, adsorbates, and experimental conditions. Roman et al. [83] demonstrated that the adsorption of caffeine on pistachio nut shell hydrochar, when processed with acidic water during hydrothermal carbonization, and that of the same sample after pyrolysis followed a Langmuir isotherm with preferably high adsorption capacities (12.95–22.6 mg/g). However, the pyrolysis of base-processed hydrochars followed the Freundlich isotherm with poor adsorption capacity. This work explored new insights, such as the excellent adsorption capacity of acid-processed hydrochars despite their lower BET surface area in comparison with base-processed hydrochars and different isotherm slopes with acid-processed hydrochars and the same sample after pyrolysis. The reason for the former finding was attributed to the development of steric hindrance, repulsive interactions, and strong resistance of base-generated functional groups. The reason behind the latter finding was the removal of OFGs on thermal treatment that was unfavorable for adsorption when high initial concentrations were used. The result suggested that despite the large pores on pyrolyzed acid-processed hydrochars, unpyrolyzed hydrochars were more promising. Further insights were also obtained by simulation studies. Liu et al. [69] applied these two models to probe the interactions between tetracycline on AC and magnetic AC from rice straw hydrochars. In comparison with the Freundlich isotherm, the Langmuir isotherm in linear form was a better-fitting model, resulting in q_m 714 mg/g for AC and 303 mg/g for magnetic AC. R_L value was within 0.02–0.04, which indicated a favorable adsorption.

Zhu et al. [93] fitted a linear Langmuir isotherm in their study of the adsorption of roxorsone on magnetic AC from sawdust hydrochars obtained at different temperatures. The maximum adsorption capacity of q_m 588 mg/g was obtained using magnetic AC derived from hydrochar obtained at 160 °C. A linear correlation between BET surface area, volumes of micropore and total pores, and the maximum adsorption capacities from the Langmuir isotherm provided the main clue to this exclusively large capacity. Chen et al. [86] prepared magnetic AC from sawdust hydrochar for tetracycline adsorption. Linear plots of the Freundlich and Langmuir equations favored the former isotherm on the basis of its high coefficient of determination. The q_m value from the Langmuir equation (423.7 mg/g) was considered the greatest among all values for all adsorbents. The magnetization barely impeded the adsorption performance of AC. Hydrothermally obtained hydrochars and their ACs have proven to be promising adsorbents. Zhu et al. [95] also obtained superior adsorption capacity in their triclosan adsorption study on γ-Fe_2O_3 carbon. The Langmuir-fitted data presented a high regression coefficient that lacked information about the Freundlich isotherm. The correlation of the different texture characteristics of ACs prepared at different temperatures with Langmuir q_m showed a linear response; in particular, micropore volume had the best correlation with q_m.

Profound research interest has long been noted in the nonlinear optimization of adsorption modeling. Ning et al. [80] prepared Fe–Mn binary oxide modified hydrochar from rice husk for the removal of E2. The nonlinear modes of the Freundlich and Langmuir equations predicted excellent fit to the isotherm data of E2. However, error values were minimum with the Langmuir model (Fig. 7). The involvement of Fe–Mn binary oxides augmented the adsorption capacity (49.7 mg/g) relative to the case of bare hydrochars (38.8 mg/g). Tian et al. [81] prepared rice husk hydrochar and montmorillonite composites for the removal of two EDCs, namely E2 and 17α ethynyl estradiol. The nonlinear form of the Langmuir model was the well fitted equation according to the regression coefficient values, and a close agreement was

Table 5
Adsorption isotherms and their parameters for the adsorption of ECs and EDCs on hydrochar/AC from lignocellulose-derived hydrochars.

Adsorbent	Pollutant	Langmuir Isotherm			Freundlich Isotherm			Experimental parameters	References
		q_m (mg/g)	K_L (L/mg)	R^2	K_F $mg^{(1-1/n)}.L^{1/n}/g$	n	R^2		
Activated carbon from hydrochars of Agave Americana fibers in combination with tannin	Tetracycline	87.21	0.42	0.968	31.26	3.82	0.775	0.5 – 400 mg/L pH 7, 50 °C, Dose 0.05, g/100 m L	[91]
Hydrochars from Argun nut shells	Diuron	833.3	0.200	0.992	149.45	0.949	0.912	10 – 40 mg/L 293 K 3 h 0.01 g/200 mL	[79]
Hydrochars from Argun nut shells	Bisphenol A	1162.79	0.956	0.989	38.36	3.729	0.979	10 – 60 mg/L 293 K 3 h 0.01 g/200 mL	[79]
Pistachio nut shells hydrochars prepared from acidic water	Caffeine	22.6	0.04	0.993	0.3	0.97	0.971	0.02 – 1 g/L 25°C 48 h Dose 0.01 g/15 mL	[83]
Montmorillonite/rice husk hydrochars	17α-ethynyl estradiol	69	1.77	0.998	37	2.7	0.915	25°C Dose 5 mg/100 m L 24 h	[81]
Montmorillonite/rice husk hydrochars	17β-estradiol	138	1.77	0.994	73	2.63	0.922	25 °C Dose 5 mg/100 m L 24 h	[81]
Magnetic activated carbons from sawdust hydrochar	Tetracycline	423.7	0.028	0.972	39.2	2.5	0.85	50 – 600 mg/L 25 °C Dose 20 mg	[86]
Rice husk based hydrochars	17β-estradiol	38.5	0.5	0.983	15.87	0.52	0.982	0.2 – 8 mg/L 28 °C Dose 5 mg	[80]
Fe-Mn loaded binary oxides on rice husk based hydrochars	17β-estradiol	49.7	0.53	0.985	22.31	0.53	0.981	0.2 – 8 mg/L 28°C Dose 5 mg	[80]
Magnetic activated carbon from sugar cane bagasse	Tetracycline				6.63	2.47	0.993	0 – 200 mg/L pH 6.8 30 °C 24 h 0.05 g/25 mL	[89]
Oxidized activated carbon from potato peel hydrochar	Pramipexole	66	0.082	0.98	8.19	1.85	0.99	0 – 200 mg/L 25 °C pH 2 dose 0.02 g/20 mL	[88]
Oxidized activated carbon from potato peel hydrochar	Dorzolamide	60	0.081	0.98	7.78	1.91	0.99	0 – 200 mg/L 25 °C pH 2 dose 0.02 g/20 mL	[88]
Magnetic activated carbon from sawdust hydrochar	Roxarsone	588.2	0.063	0.99	–	–	–	50 – 500 mg/L 25 °C Dose 0.02 g	[93]
Phosphoric acid activated carbon from orange peel hydrochars	Diclofenac	0.211 mmol/g	27.5 L/mmol	0.981	0.203 [(mmol/g)L/mmol)$_f^n$]	0.2	0.971	0.05 – 2 mmol/L 25°C 0.015 g/30 mL pH 7	[5]
Phosphoric acid activated carbon from orange peel hydrochars	Salicylic acid	0.66 mmol/g	10.9 L/mmol	0.978	0.63[(mmol/g)L/mmol)$_f^n$]	0.28	0.941	pH 2 0.05 – 2 mmol/L 25 °C 0.015 g/30 mL	[5]
Phosphoric acid activated carbon from orange peel hydrochars	Flurbiprofen	0.61 mmol/g	83.9 L/mmol	0.981	1.45[(mmol/g)L/mmol)$_f^n$]	0.37	0.985	pH 2 0.05 – 2 mmol/L 25 °C 0.015 g/30 mL	[5]
Magnetic activated carbon from Salix psammophila	Triclosan	892.9	0.69	0.98	–	–	–	10 – 50 mg/L 303 K Dose 500 mg/L	[95]
Activated carbon from Salix psammophila	Tetracycline	–	–	–	8.57	0.404	0.996	5 – 50 mg/L 30°C 4 days Dose 0.04 g/40 mL	[115]
Magnetic activated carbon from salix psammophila	Tetracycline	25.4	1.08	0.85	11.78	4.34	0.99	5 – 80 mg/L 303K Dose 0.05 g/50 m L 5 days	[110]
Magnetic activated carbon from rice straw hydrochar	Tetracycline	303	0.89	0.99	150	4.68	0.91	10 – 50 mg/L 298K	[69]
Activated carbon from Rice straw hydrochar	Tetracycline	714	0.52	0.97	232	2.25	0.64	10 – 50 mg/L 298 K	[69]

found between the calculated values and the experimental q_m values; the adsorption capacity for E2 (138 mg/g) was the highest, followed by that for 17α ethynyl estradiol (69 mg/g). However, the concentration range selected was small (0.2–8 mg/L) possibly because of the limited solubilities of both solutes that otherwise could provide a deviation from Langmuir to Freundlich. The fabrication of these composites was claimed as an easy and cheap method with superior adsorption capacities for the two model pollutants in comparison with previously used materials.

Fernandez et al. [5] studied the adsorption of emerging pharmaceuticals (diclofenac, salicylic acid, and flurbiprofen) on ACs achieved by air and phosphoric acid treatment of orange peel hydrochars. An isotherm study was performed at pH 7 in the case of diclofenac and at pH 2 in the cases of salicylic acid and flurbiprofen in a nonlinear mode. The Freundlich equation best fitted with the adsorption data of diclofenac on air AC, whereas the Langmuir isotherm was the most appropriate when using phosphoric acid AC. The adsorption capacities in both cases (0.164 and 0.211 mmol/g) were claimed to be higher than those of other biomass-based ACs. In the case of salicylic acid and flurbiprofen, the experimental data best fitted the Langmuir isotherm. In some cases, the Freundlich model was the preferable isotherm, as explained by Kyzas and Deliyanni [88], who applied nonlinear Freundlich and Langmuir equations for their study of the adsorption of two pharmaceuticals, namely, dorzolamide and pramipexole, on oxidized ACs prepared via hydrothermal and pyrolysis treatments. Both drugs followed the Freundlich model, with pramipexole having higher adsorption capacity than dorzolamide did. The ACs prepared from hydrochars showed greater adsorption capacities than those prepared from biochars of the same precursor via pyrolysis. Their study showed that preparation methods greatly affect the adsorption performances of resulting ACs. The Freundlich isotherm was again the best fitted model on the basis of the experimental data of tetracycline adsorption in magnetic AC from *Salix psammophila* with a Langmuir adsorbed amount of 25.4 mg/g as a result of the many graphitic layers and porous texture. The R_L values within 0.011–0.16 also suggested a favorable adsorption process [110]. Rattanachueskul et al. [89] studied the adsorption performance of magnetic AC derived from sugar cane bagasse for removing tetracycline. The Freundlich isotherm model was the better fitted model with a value of $n = 2.47$, which indicated a heterogeneous adsorption that further strengthened the assumption that the resulting adsorbent possessed a large number of heterogeneous sites.

However, relying on isotherms for the prediction of adsorption mechanisms is not the exclusive method for demonstrating solute–-adsorbent interactions. Some advanced computational modeling studies, along with advanced characterization tools, should be deduced to learn the effect of variables like pH, molecular geometries, and surface and interaction energies on the mechanisms of adsorption [83]. Another remarkable study is that conducted by Flora et al. [98], who investigated the influence of hydrochars with and without washing for removal of atrazine. The calculation of the binding energies between the atrazine hydrochars showed low favorable binding energies when atrazine was parallel to the hydrochar plane. The adsorptive capacities of the hydrochars obtained by acetone washing were superior to those of the hydrochars without washing. This deviation in adsorption can be related to the less preferable attraction energy of atrazine for hydrochars without washing with weakly associated alkyl groups on the surface relative to hydrochars with washing.

According to Table 5, Langmuir model well represents the adsorption isotherm data of most EDC/EC pollutants on hydrochars and their derived ACs. Freundlich model is also applicable in some cases. From the parameters of both models the adsorption process is favorable. In the literature, the adsorption capacities of different hydrochars or the ACs derived from them for EDC/EC removal were claimed to be superior to those of other reported materials [5,79,81,86,95], thereby suggesting that hydrochars may open a new horizon in carbon chemistry as their interesting surface features and low-cost preparation methods supersede the features of commercially available ACs ; the use of such material encourages further investigations into the removal of other wide varieties of pollutants. The commercialization and implementation of the method in practical settings are encouraged in the current industrialization era.

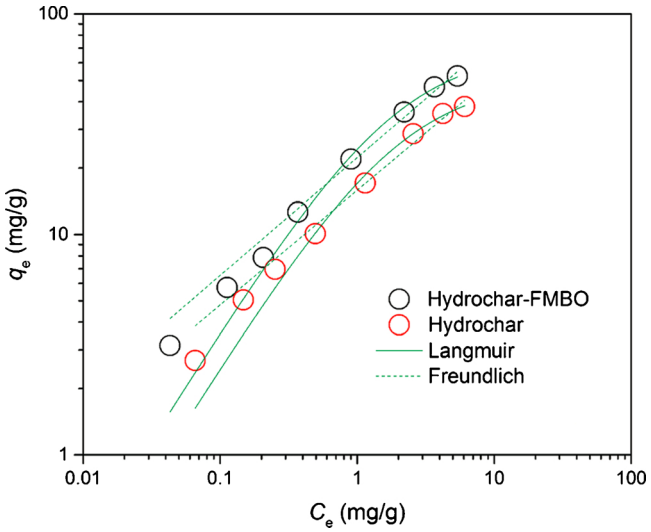

Fig. 7. Adsorption isotherm data and fitted models for 17β-estradiol on raw hydrochar and Fe-Mn oxide modified hydrochar [80].

8. Reusability of adsorbents

The worth of any adsorbent material can be appraised if the material concerned is economic, efficient, and long-lasting. Reusability is one of the important aspects in this technology because this property may help reduce the cost of adsorbents, minimize disposal issues, and prevent the laborious work needed to resynthesize fresh adsorbent materials for the consecutive adsorption system. Our extensive literature survey on the topic has revealed the limited number of studies on the reusability of lignocellulose-based hydrochars, their composites, and the ACs derived from them. Good desorption depends upon the type of interactions and solvents. Rattanachueskul et al. [89] demonstrated that magnetic carbon from sugar cane bagasse hydrochar can be reused for tetracycline adsorption when treated with 25 mL of 0.1 M NaOH solution. As a normal trend, the adsorption efficiency declined after every cycle (from 81.84 % to 57.27 %), thereby confirming strong interactions between tetracycline and the adsorbent.

In an existing study, ACs from potato peel hydrochars obtained after hydrothermal treatment and oxidation showed good reusable performance, that is, reusability of up to 20 times with desorption carried at an optimum pH level of 10, in dorzolamide and pramipexole removal [88]. The work reported only an 11 % decline in initial adsorption efficiency. This decreasing trend was attributed to the progressive saturation of the active sites and the degradation of the materials due to the highly basic pH and blockage of active sites.

Meanwhile, Fe–Mn binary oxide-loaded rice husk-based hydrochars showed good reusability of up to five times for 6 mg/L E2 removal. The desorption medium used was acetone/water mixture in the ratio of 1:1 (v/v) based on a high octanol–water partitioning coefficient in acetone [80]. Tian et al. [81] performed a regeneration study of montmorillonite rice husk hydrochar composites with 20 mL ethanol, which were washed with water multiple times and then dried. The regenerated adsorbent retained 82 % and 80.2 % of the initial sorption capacities for E2 and 17α ethynyl estradiol, respectively. Excellent stability and reusability were found by Zbair et al. [79] using Argan nut shell hydrochars for the removal of diuron and bisphenol A. The desorption of the retained pollutants was conducted using ethanol. The

frequency of recycling (up to 5 times) had no significant effect on adsorption efficiency, and the material could sustain its removal efficiency for bisphenol A (88 %) and diuron (94 %), as shown in Fig. 8. Only a 5% decline was reported in the efficiency of bisphenol A removal, whereas a 1% decline was reported for diuron for five consecutive adsorption–desorption cycles.

Hydrochars and their derived ACs can be efficiently reutilized for several cycles after regeneration by NaOH and organic agents. Ideally, a desorbing agent should be neither too punitive nor too expensive for the regeneration of adsorbents to affect adsorbents' efficiency or technology. From the above discussions, we observed that mostly organic solvents were used for the desorption of studied pollutants that are expensive and volatile. This approach could affect process efficiency from the ecological and economic perspectives. A systematic study with green solvents for the regeneration of spent adsorbents is necessary to achieve a successful adsorption of these pollutants. Moreover, the fate of these desorbing agents remains undecided; they are mostly disposed to the sink and may thus cause secondary pollution. Such gaps should be considered, and recyclability techniques should be developed to regenerate desorbing solvents and recollect desorbed pollutants that may be removed or returned to the manufacturing industry. Only Zbair et al. [79] addressed some alternative solutions to the present dilemma; that is, the incineration of exhausted adsorbents and conversion of retained pollutants to less harmful byproducts. However, such a study requires proper waste management techniques and transport facilities that should be considered by environmental protection agencies.

9. Conclusions and future perspectives

In this review, we focused on the recent studies on the applications of lignocellulose-based hydrochars and their post-hydrothermally treated ACs. This work invokes the slogan, "treatment of waste by waste," and may serve as a beacon in green chemistry. These hydrochars can successfully replace commercially available resins and ACs for the removal of ECs and EDCs. Post-treated ACs from hydrochar precursors have shown promising and improved results relative to their precursors because of their large surface area and high porosity. The mechanism of adsorption greatly depends upon experimental conditions, and adsorption is controlled by a myriad of interactions, such as electrostatic, hydrophobic, and π-π interactions; pore filling; hydrogen bonding; and intercalations. The use of hydrochars and ACs in the removal of ECs and EDCs has elicited keen interest in the last few years due to the great adsorption capacities that they offer. Adsorption kinetics is a pseudo-second-order equation in all studies, and intraparticle diffusion is not the sole rate-limiting step. Adsorption isotherms are frequently of Langmuir type, but some studies cited the Freundlich isotherm as the best one. Efficient regeneration and reusability profiles have been exhibited for hydrochars and their derived ACs. Some issues remain unaddressed and must be considered to broaden the scope of these new emerging materials.

The studies discussed in the current review were mainly based on the batch system for determining the adsorption performance of different hydrochars and their ACs. Thus, carrying out column, pilot, full-scale, and multi-component adsorption studies is useful to appraise these adsorbents in real applications that involve interfering substances. The adsorption behavior of other EDCs and ECs, such as phthalates, parabens, DDT, herbicides, and pesticides, should also be investigated to apply these new materials to practical settings. The proper and careful study of the exact adsorption mechanism is also required in designing a suitable adsorbent that depends on the complex structure of different ECs and EDCs. Furthermore, the magnetization of porous ACs may enhance their adsorption efficiency relative to bare hydrochars. The regeneration and reusability of hydrochar and AC adsorbents using nontoxic and cheap solvents should be investigated to make the process economically viable. Cost analysis studies and the practical implementation of these adsorbents should also be given adequate attention to strengthen their replacement with ACs.

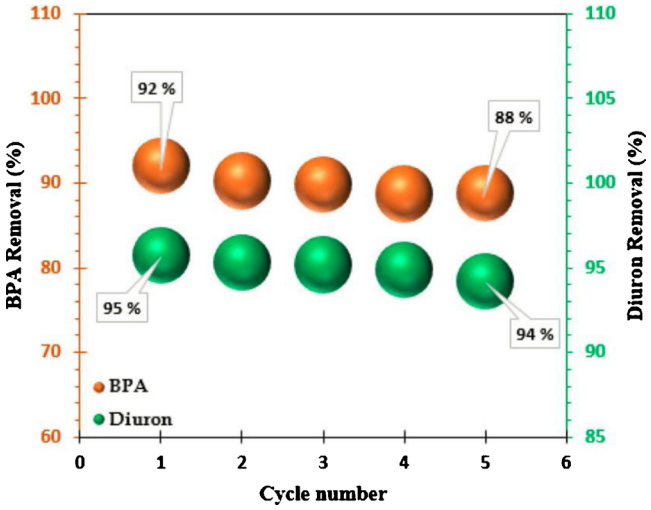

Fig. 8. Reusability of Argan nut shell derived hydrochar for the adsorption of bisphenol A and diuron [79].

Other gaps pointed out in the current review include the development of a systematic classification to distinguish ECs and EDCs and the establishment of proper guideline values. Strict measures should also be taken to frame legislation on the release of these contaminants from industrial wastes. An accurate, precise, and sensitive standard analytical method is required for the simultaneous determination of well-known EDCs and ECs at their trace levels. Proper knowledge of the mechanism of hydrochar formation from complex lignocellulose biomass is equally important. The use of green activating agents for the preparation of ACs should be studied. Owing to the frequent presence of these toxic unregulated pollutants at alarming levels, wastewater treatments should be upgraded to resolve these rapid-growing problems by either modifying the membrane materials with such novel and sustainable materials as their components or replacing commercially applied ACs to treat recalcitrant ECs and EDCs. Such attempts may improve water quality and substantially reduce the costs for expensive membranes. Hydrochars and their derived ACs may leave some adverse effects; therefore, an evaluation of their ecotoxicity and an assessment of their environmental influences are strongly recommended.

Declaration of Competing Interest

The authors declare that they have no known competing financial interests or personal relationships that could have appeared to influence the work reported in this paper.

Acknowledgement

The publication of this article was funded by the Qatar National Library.

References

[1] N. Chaukura, B.B. Mamba, S.B. Mishra, Porous materials for the sorption of emerging organic pollutants from aqueous systems: the case for conjugated microporous polymers, J. Water Process Eng. 16 (2017) 223–232.
[2] Commission of the European Communities, The Implementation of the Community Strategy for Endocrine Disrupters: A Range of Substances Suspected of Interfering With the Hormone Systems of Humans and Wildlife, COM [1999], Vol. 706, (2001) pp. 45.
[3] M. Sevilla, A.B. Fuertes, The production of carbon materials by hydrothermal carbonization of cellulose, Carbon 47 (2009) 2281–2289.
[4] Y. Xue, B. Gao, Y. Yao, et al., Hydrogen peroxide modification enhances the ability of biochar (hydrochar) produced from hydrothermal carbonization of peanut hull to remove aqueous heavy metals: batch and column studies, Chem. Eng. J. 200-

202 (2012) 673–680.
[5] M.E. Fernandez, B. Ledesma, S. Roman, P.R. Bonelli, A.L. Cukiermann, Development and characterization of activated hydrochars from orange peels as potential adsorbents for emerging contaminants, Bioresour. Technol. 183 (2015) 221–228.
[6] P. Zhao, Y. Shen, S. Ge, et al., Clean solid biofuel production from high moisture content waste biomass employing hydrothermal treatment, Appl. Energy 131 (2014) 345–367.
[7] M.M. Titirici, R.J. White, C. Falco, M. Sevilla, Black perspectives for a green future: hydrothermal carbons for environment protection and energy storage, Energy Environ. Sci. 5 (2012) 6796–6822.
[8] M.T. Reza, J. Andert, B. Wirth, et al., Hydrothermal carbonization of biomass for energy and crop production, Appl. Bioenergy 1 (2014) 11–29.
[9] L. Ding, B. Zou, Y. Li, et al., The production of hydrochar based hierarchical porous carbons for use as electrochemical supercapacitor electrode materials, Colloids Surf. A Physicochem. Eng. Asp. 423 (2013) 104–111.
[10] K.Y. Park, K. Lee, D. Kim, Characterized hydrochar of algal biomass for producing solid fuel through hydrothermal carbonization, Bioresour. Technol. 258 (2018) 119–124.
[11] E. Atallah, W. Kwapinski, M.N. Ahmad, J.J. Leahy, J. Zeaiter, Effect of water-sludge ratio and reaction time on the hydrothermal carbonization of olive oil mill wastewater treatment: hydrochar characterization, J. Water Process Eng. 31 (2019) 100813.
[12] G.K. Parshetti, S. Chowdhury, R. Balasubramanian, Hydrothermal conversion of urban food waste to chars for removal of textile dyes from contaminanted waters, Bioresour. Technol. 161 (2014) 310–319.
[13] Y. Dai, Q. Sun, W. Wang, et al., Utilization of agricultural waste as adsorbent for the removal of contaminants: a review, Chemosphere 211 (2018) 235–253.
[14] Y. Dai, N. Zhang, C. Xing, et al., The adsorption, regeneration and engineering applications of biochar for removal organic pollutants: a review, Chemosphere 223 (2019) 12–27.
[15] A. Bhatnagar, I. Anastopoulus, Adsorptive removal of bisphenol A (BPA) from aqueous solution: a review, Chemosphere 168 (2017) 885–902.
[16] S. Kim, C.M. Park, M. Jang, et al., Aqueous removal of inorganic and organic contaminants by graphene-based nanoadsorbents: a review, Chemosphere 212 (2018) 1104–1124.
[17] M.B. Ahmed, J.L. Zhou, H.H. Ngo, et al., Progress in the biological and chemical treatment technologies for emerging contaminant removal from wastewater: a critical review, J. Hazard. Mater. 323 (2017) 274–298.
[18] N.H. Tran, M. Reinhard, K.Y.-H. Gin, Occurrence and fate of emerging contaminants in municipal wastewater treatment plants from different geographical regions-a review, Water Res. 133 (2018) 182–207.
[19] M. Taheran, M. Naghdi, S.K. Brar, M. Verma, R.Y. Surampalli, Emerging contaminants: here today, there tomorrow, Environ. Nanotechnol. Mon. Manage. 10 (2018) 122–126.
[20] D.W. Kolpin, E.T. Furlong, M.T. Meyer, E.M. Thurman, S.D. Zaugg, L.B. Barber, H.T. Buxton, Pharmaceuticals, hormones, and other organic wastewater contaminants in US streams, 1999-2000: a national reconnaissance, Environ. Sci. Technol. 36 (2002) 1202–1211.
[21] K. Kümmerer, Drugs in the environment: emission of drugs, diagnostic aids and disinfectants into wastewater by hospitals in relation to other sources-a review, Chemosphere 45 (2001) 957–969.
[22] L.S. Shore, M. Shemesh, Naturally produced steroid hormones and their release into the environment, Pure Appl. Chem. 75 (2003) 1859–1871.
[23] I.J. Buerge, H.R. Buser, M. Kahle, M.D. Müller, T. Poiger, Ubiquitous occurrence of the artificial sweetener acesulfame in the aquatic environment: an ideal chemical marker of domestic wastewater in groundwater, Environ. Sci. Technol. 43 (2009) 4381–4385.
[24] D.J. Lapworth, N. Baran, M.E. Stuart, R.S. Ward, Emerging organic contaminants in groundwater: a review of sources, fate and occurrence, Environ. Pollut. 163 (2012) 287–303.
[25] S. Sifakis, Androutsopoulos, A.M. Tsatsakis, et al., Human exposure to endocrine disrupting chemicals: effects on the male and female reproductive systems, Environ. Toxicol. Pharmacol. 51 (2017) 56–70.
[26] J.O. Tijani, O.O. Fatoba, L.F. Petrik, A review of pharmaceuticals and endocrine-disrupting compounds: sources, effects, removal, and detections, Water Air Soil Pollut. 224 (2013) 1770.
[27] Y. Jia, M. Hammers-Wirtz, et al., Effect-based and chemical analyses of agonistic and antagonistic endocrine disruptors in multiple matrices of eutrophic freshwaters, Sci. Total Environ. 651 (2019) 1096–1104.
[28] N. Salgueiro-Gonzalez, M.J. Lopez de Alda, S. Muniategue-Lorenzo, et al., Analysis and occurrence of endocrine-disrupting chemicals in airborne particles, Trends Analyt. Chem. 66 (2015) 45–52.
[29] J.S. Helm, M. Nishioka, J.G. Brody, et al., Measurement of endocrine disrupting and asthma-associated chemicals in hair products used by Black women, Environ. Res. 165 (2018) 448–458.
[30] J. Annamalai, V. Namasivayam, Endocrine disrupting chemicals in the atmosphere: their effects on humans and wildlife, Environ. Int. 76 (2015) 78–97.
[31] I.-H. Acir, K. Guenther, Endocrine-disrupting metabolites of alkylphenol ethoxylates-A critical review of analytical methods, environmental occurences, toxicity and regulation, Sci. Total Environ. 635 (2018) 1530–1546.
[32] M. Zhong, P. Yin, L. Zhao, Nonylphenol and octylphenol in riverine waters and surface sediments of the Pearl River estuaries, South China: occurrence, ecological and human health risks, Water Sci. Technol. Water Supply 17 (2017) 1070–1079.
[33] K. Gunther, T. Racker, R. Bohme, An isomer-specific approach to endocrine disrupting Nonylphenol in infant food, J. Agric. Food Chem. 65 (2017) 1247–1254.
[34] Z. Hao, Y. Xiao, L. Jiang, et al., Simultaneous determination of bisphenol a, bisphenol F, 4-Nonylphenol, 4-n-Nonylphenol, and octylphenol in grease-rich food by Carb/PSA solid-phase extraction combined with high-performance liquid chromatography tandem mass spectrometry, Food Anal. Methods 11 (2018) 589–597.
[35] Z.-H. Liu, Y. Kanjo, S. Mizutani, Removal mechanisms for endocrine disrupting compounds (EDCs) in wastewater treatment – physical means, biodegradation, and chemical advanced oxidation: a review, Sci. Total Environ. 407 (2009) 731–748.
[36] T. Saeed, N. Al-Jandal, A. Abusam, et al., Sources and levels of endocrine disrupting compounds (EDCs) in Kuwait's coastal areas, Mar. Pollut. Bull. 118 (2017) 407–412.
[37] H. Arfaeinia, M. Fazlzadeh, F. Taghizadeh, et al., Phthalate acid esters (PAEs) accumulation in coastal sediments from regions with different land use configuration along the Persian Gulf, Ecotox. Environ. Safe. 169 (2019) 496–506.
[38] S.-Q. Tian, R.-Y. Zhao, Z.-C. Chen, Review of the pretreatment and bioconversion of lignocellulosic biomass from wheat straw materials, Renew. Sust. Energ. Rev. 91 (2018) 483–489.
[39] J. Hoarau, Y. Caro, I. Grondin, T. Petit, Sugarcane vinasse processing: toward a status shift from waste to valuable resource. A review, J. Water Process Eng. 24 (2018) 11–25.
[40] A. Arvelo-Gallegos, Z. Ahmad, M. Asgher, et al., Lignocellulose: a sustainable materials to produce value-added product with a zero waste approach-a review, Int. J. Biol. Macromol. 99 (2017) 308–318.
[41] G. Kabir, B.H. Hameed, Recent progress on catalytic pyrolysis of lignocellulosic biomass to highgrade bio-oil and bio-chemicals, Renew. Sust. Energ. Rev. 70 (2017) 945–967.
[42] X. Han, Y. Guo, X. Liu, Catalytic conversion of lignocellulosic biomass into hydrocarbons: a mini review, Catal. Today 319 (2019) 2–13.
[43] S.S. Hassan, G.A. Williams, A.K. Jaiswal, Emerging technologies for the pretreatment of lignocellulosic biomass, Bioresour. Technol. 262 (2018) 310–318.
[44] P. Burguete, A. Corma, M. Hitzl, et al., Fuel and chemicals from wet lignocellulosic biomass waste streams by hydrothermal carbonization, Green Chem. 18 (2016) 1051–1060.
[45] A. Jain, R. Balasubramanian, M.P. Srinivasan, Hydrothermal conversion of biomass waste to activated carbon with high porosity: a review, Chem. Eng. J. 283 (2016) 789–805.
[46] A. Salimbeni, Biobased Char Market Potentials, European Biomass Industry Association, 2015.
[47] T. Wang, Y. Zhai, Y. Zhu, C. Li, G. Zeng, A review of the hydrothermal carbonization of biomass waste for hydrochar formation: process conditions, fundamentals and physicochemical properties, Renew. Sust. Energ. Rev. 90 (2018) 223–247.
[48] H. Huang, X. Yuan, G. Zeng, H. Zhu, H. Li, Z. Liu, H. Jiang, L. Leng, W. Bi, Quantitative evaluation of heavy metals' pollution hazards in liquefaction residues of sewage sludge, Bioresour. Technol. 102 (2011) 10346–10351.
[49] T. Liu, Z. Liu, Q. Zheng, Effect of hydrothermal carbonization on migration and environmental risk of heavy metals in sewage sludge during pyrolysis, Bioresour. Technol. 247 (2018) 282–290.
[50] N. Saha, A. Saba, M.T. Reza, Effect of hydrothermal carbonization temperature on pH, dissociation constants, and acidic functional groups on hydrochar from cellulose and wood, J. Anal. Appl. Pyrol. 137 (2019) 138–145.
[51] D. Zhang, F. Wang, X. Shen, et al., Comparison study on fuel properties of hydrochars produced from corn stalk and corn stalk digestate, Energy 165 (2018) 527–536.
[52] Q. Ma, L. Han, G. Huang, Effect of water-washing of wheat straw and hydrothermal temperature on its hydrochar evolution and combustion properties, Bioresour. Technol. 269 (2018) 96–103.
[53] A.M. Smith, S. Singh, A.B. Ross, Fate of inorganic material during hydrothermal carbonisation of biomass: influence of feedstock on combustion behaviour of hydrochar, Fuel 169 (2016) 135–145.
[54] M. Wilk, A. Magdziarz, K. Jayaraman, et al., Hydrothermal carbonization characteristics of sewage sludge and lignocellulosic biomass. A comparative study, Biomass Bioenerg. 120 (2019) 166–175.
[55] I. Oliveira, D. Blohse, H.G. Ramke, Hydrothermal carbonization of agricultural residues, Bioresour. Technol. 142 (2013) 138–146.
[56] Y.O. Donar, E. Çag ˘lar, A. Sınag, Preparation and characterization of agricultural waste biomass based hydrochars, Fuel 183 (2016) 366–372.
[57] H. Yang, R. Yan, H. Chen, D.H. Lee, C. Zheng, Characteristics of hemicellulose, cellulose and lignin pyrolysis, Fuel 86 (2007) 1781–1788.
[58] Y. Li, N. Tsend, T. Li, et al., Microwave assisted hydrothermal preparation of rice straw hydrochars for adsorption of organics and heavy metals, Bioresour. Technol. 273 (2019) 136–143.
[59] M.T. Reza, E. Rottler, L. Herklotz, et al., Hydrothermal carbonization (HTC) of wheat straw: influence of feed water pH prepared by acetic acid and potassium hydroxide, Bioresour. Technol. 182 (2015) 336–344.
[60] Q. Lang, B. Zhang, Z. Liu, et al., Co-hydrothermal carbonization of corn stalk and swine manure: combustion behavior of hydrochar by thermogravimetric analysis, Bioresour. Technol. 271 (2019) 75–83.
[61] X. Zhang, L. Zhang, A. Li, Hydrothermal co-carbonization of sewage sludge and pinewood sawdust for nutrient-rich hydrochar production: synergistic effects and products characterization, J. Environ. Manage. 201 (2017) 52–62.
[62] Q. Lang, Y. Guo, Q. Zheng, et al., Co-hydrothermal carbonization of lignocellulosic biomass and swine manure: hydrochar properties and heavy metal transformation behavior, Bioresour. Technol. 266 (2018) 242–248.
[63] Z.M.A. Bundhoo, Microwave-assisted conversion of biomass and waste materials

to biofuels, Renew. Sust. Energ. Rev. 82 (2018) 1149–1177.
[64] Y. Shao, Y. Long, H. Wang, et al., Hydrochar derived from green waste by microwave hydrothermal carbonization, Renew. Energy 135 (2019) 1327–1334.
[65] T. Maneerung, J. Liew, Y. Dai, et al., Activated carbon derived from carbon residue from biomass gasification and its application for dye adsorption: kinetics, isotherms and thermodynamic studies, Bioresour. Technol. 200 (2016) 350–359.
[66] M. Sevilla, G.A. Ferrero, A.B. Fuertes, Beyond KOH activation for the synthesis of superactivated carbons from hydrochars, Carbon 114 (2017) 50–58.
[67] M. Sevilla, A.B. Fuertes, R. Mokaya, High density hydrogen storage in super activated carbons from hydrothermally carbonized renewable organic materials, Energy Environ. Sci. 4 (2011) 1400–1410.
[68] L. Wang, Y. Guo, B. Zou, et al., High surface area porous carbons prepared from hydrochars by phosphoric acid activation, Bioresour. Technol. 102 (2011) 1947–1950.
[69] Y. Liu, X. Zhu, F. Qian, et al., Magnetic activated carbon prepared from rice straw-derived hydrochar for triclosan removal, RSC Adv. 4 (2014) 63620–63626.
[70] M.A. Islam, M.J. Ahmed, W.A. Khanday, M. Asif, B.H. Hameed, Mesoporous activated carbon prepared from NaOH activation of rattan (Lacosperma secundiflorum) hydrochar for methylene blue removal, Ecotox. Environ. Safe. 138 (2017) 279–285.
[71] M.A. Islam, M.J. Ahmed, W.A. Khanday, M. Asif, B.H. Hameed, Mesoporous activated coconut shell derived hydrochar prepared via hydrothermal carbonization-NaOH activation for methylene blue adsorption, J. Environ. Manage. 203 (2017) 237–244.
[72] M.A. Islam, I.A.W. Tan, A. Benhouria, M. Asif, B.H. Hameed, Mesoporous and adsorptive properties of palm date seed activated carbon prepared via sequential hydrothermal carbonization and sodium hydroxide activation, Chem. Eng. J. 270 (2015) 187–195.
[73] X. Zhu, Y. Liu, C. Zhou, et al., Novel and high-performance magnetic carbon composite prepared from waste hydrochar for dye removal, ACS sustain, Chem. Eng. 2 (2014) 969–977.
[74] A. Jain, R. Balasubramanian, M.P. Srinivasan, Production of high surface area mesoporous activated carbons from waste biomass using hydrogen peroxide-mediated hydrothermal treatment for adsorption applications, Chem. Eng. J. 273 (2015) 622–629.
[75] A. Jain, R. Balasubramanian, M.P. Srinivasan, Tuning hydrochar properties for enhanced mesopore development in activated carbon by hydrothermal carbonization, Microporous Mesoporous Mater. 203 (2015) 178–185.
[76] A.R. Guastalli, J. Labanda, J. Llorens, Separation of phosphoric acid from an industrial rinsing water by means of nanofiltration, Desalination 243 (2009) 218–228.
[77] X.-f Tan, S.-b Liu, Y.-g Liu, Biochar as potential sustainable precursors for activated carbon production: multiple applications in environmental protection and energy storage, Bioresour. Technol. 227 (2017) 359–372.
[78] K.Y. Foo, B.H. Hameed, Potential of jackfruit peel as precursor for activated carbon prepared by microwave induced NaOH activation, Bioresour. Technol. 112 (2012) 143–150.
[79] M. Zbair, M. Bottlinger, K. Ainassaari, et al., Hydrothermal Carbonization of Argan Nut Shell: Functional Mesoporous Carbon with Excellent Performance in the Adsorption of Bisphenol a and Diuron, Waste Biomass Valori, (2018) https://doi.org/10.1007/s1264 9-018-00554-0.
[80] Q. Ning, Y. Liu, S. Liu, et al., Fabrication of hydrochar functionalized Fe-Mn binary oxide nanocomposites: characterization and 17β-estradiol removal, RSC Adv. 7 (2017) 37122–37129.
[81] S. Tian, Y. Liu, S. Liu, et al., Hydrothermal synthesis of montmorillonite/hydrochar nanocomposites and application for 17β-estradiol and 17α-ethynylestradiol removal, RSC Adv. 8 (2018) 4273–4283.
[82] E. Weidemann, M. Niinipuu, J. Fick, S. Jansson, Using carbonized low-cost materials for removal of chemicals of environmental concern from water, Environ. Sci. Pollut. Res. 25 (2018) 15793–15801.
[83] S. Román, B. Ledesma, A. Álvarez, C. Herdes, Towards sustainable micro-pollutants'removal from wastewaters: caffeine solubility, self diffusion and adsorption studies from aqueous solutions into hydrochars, Mol. Phys. (2018), https://doi.org/10.1080/00268976.2018.1487597.
[84] N. Eibisch, R. Schroll, R. Fuβ, et al., Pyrochars and hydrochars differently alter the sorption of the herbicide isoproturon in an agricultural soil, Chemosphere 119 (2015) 155–162.
[85] J. Deng, X. Li, X. Wei, et al., Sulfamic acid modified hydrochar derived from sawdust for removal of benzotriazole and Cu(II) from aqueous solution: adsorption behavior and mechanism, Bioresour. Technol. 290 (2019) 121765.
[86] S.Q. Chen, Y.L. Chen, H. Jiang, Slow pyrolysis magnetization of hydrochar for eff ;ective and highly stable removal of tetracycline from aqueous solution, Ind. Eng. Chem. Res. 56 (2017) 3059–3066.
[87] H. Li, J. Hu, Y. Cao, et al., Development and assessment of a functional activated fore-modified bio-hydrochar for amoxicillin removal, Bioresour. Technol. 246 (2017) 168–175.
[88] G.Z. Kyzas, E.A. Deliyanni, Modified activated carbons from potato peels as green environmental-friendly adsorbents for the treatment of pharmaceutical effluents, Chem. Eng. Res. Des. 97 (2015) 135–144.
[89] N. Rattanachueskul, A. Saning, S. Kaowphong, N. Chumha, L. Chuenchom, Magnetic carbon composites with a hierarchical structure for adsorption of tetracycline, prepared from sugarcane bagasse via hydrothermal carbonization coupled with simple heat treatment process, Bioresour. Technol. 226 (2017) 164–172.
[90] M. Puccini, E. Stefanelli, A.L. Tasca, S. Vitolo, Pollutant removal from gaseous and aqueous phases using hydrochar-based activated carbon, Chem. Eng. Trans. 67 (2018) 637–642.
[91] T. Selmi, A. Sanchez-Snachez, P. Gaddoneix, et al., Tetracycline removal with activated carbons produced from hydrothermal carbonisation of Agave americana fibers and mimosa tannin, Ind. Crops Prod. 115 (2018) 146–157.
[92] F. Suo, G. Xie, J. Zhang, et al., A carbonized sieve –like corn straw cellulose-graphene oxide composite for organophosphorus pesticide removal, RSC Adv. 8 (2018) 7735–7743.
[93] X. Zhu, F. Qian, Y. Liu, et al., Environmental performances of hydrochar-derived magnetic carbon composite affected by its carbonaceous precursor, RSC Adv. 5 (2015) 60713–60722.
[94] X. Zhu, F. Qian, Y. Liu, et al., Controllable synthesis of magnetic carbon composites with high porosity and strong acid resistance from hydrochar for efficient removal of organic pollutants: an overlooked influence, Carbon 99 (2016) 338–347.
[95] X. Zhu, Y. Liu, G. Luo, et al., Facile fabrication of magnetic carbon composites from hydrochar via simultaneous activation and magnetization for triclosan adsorption, Environ. Sci. Technol. 48 (2014) 5840–5848.
[96] K. Sun, K. Ro, M. Guo, et al., Sorption of bisphenol A, 17a-ethinyl estradiol and phenanthrene on thermally and hydrothermally produced biochars, Bioresour. Technol. 102 (2011) 5757–5763.
[97] S. Shi, Y. Fan, Y. Huang, Facile low temperature hydrothermal synthesis of magnetic mesoporous carbon nanocomposite for adsorption removal of ciprofloxacin antibiotics, Ind. Eng. Chem. Res. 52 (2013) 2604–2612.
[98] J.F.R. Flora, X. Lu, L. Li, et al., The effects of alkalinity and acidity of process water and hydrochar washing on the adsorption of atrazine on hydrothermally produced hydrochar, Chemosphere 93 (2013) 1989–1996.
[99] M.A. Ahsan, M.T. Islam, C. Hernandez, et al., Biomass conversion of saw dust to a functionalized carbonaceous materials for the removal of Tetracycline, Sulfamethoxazole and Bisphenol A from water, J. Environ. Chem. Eng. 6 (2018) 4329–4338.
[100] S. Lagergren, About the theory of so-called adsorption of soluble substances, Kungliga Svenska Vetenskapsakademiens 4 (1898) 1–39 Band 24.
[101] W. Rudzinski, W. Plazinski, Studies of the kinetics of solute adsorption at solid/solution interfaces: on the possibility of distinguishing between the diffusional and the surface reaction kinetic models by studying the pseudo-first order kinetics, J Phys Chem C 111 (2007) 15100–15110.
[102] Y.S. Ho, G. McKay, The sorption of Pb (II) ions on peat, Water Res. 33 (1999) 578–584.
[103] G. McKay, Y.S. Ho, J.C.Y. Ng, Biosporption of copper from waste waters: a review, Sep Purif Methods 28 (1999) 87–125.
[104] Y.S. Ho, G. McKay, Pseudo-second order model for sorption processes, Process Biochem. 34 (1999) 451–465.
[105] K.L. Tan, B.H. Hameed, Insight into the adsorption kinetics models for the removal of contaminants from aqueous solutions, J. Taiwan Inst, Chem. Eng. 74 (2017) 25–48.
[106] S. Roginsky, Y.B. Zeldovich, The catalytic oxidation of carbon monoxide on manganese dioxide, Acta Phys Chem USSR 1 (1934) 554.
[107] W.J. Weber, J.C. Morris, Kinetics of adsorption on carbon from solution, J Sanit Eng Div 89 (1963) 31–60.
[108] W. Plazinski, W. Rudzinski, A. Plazinska, Theoretical models of sorption kinetics including a surface reaction mechanism: a review, Adv. Colloid Interface Sci. 152 (2009) 2–13.
[109] A.S. Mestre, E. Tyszko, M.A. Andrade, et al., Sustainable activated carbons prepared from a sucrose-derived hydrochar: remarkable adsorbents for pharmaceutical compounds, RSC Adv. 5 (2015) 19696–19707.
[110] X. Zhu, Y. Liu, F. Qian, et al., Preparation of magnetic porous carbon from waste hydrochar by simultaneous activation and magnetization for tetracycline removal, Bioresour. Technol. 154 (2014) 209–214.
[111] G. Limousin, J.P. Gaudet, L. Charlet, S. Szenknect, V. Barthes, M. Krimissa, Sorption isotherms: are view on physical bases, modeling and measurement, Appl. Geochem. 22 (2007) 249–275.
[112] I. Langmuir, The constitution and fundamental properties of solids and liquids, J. Am. Chem. Soc. 38 (1916) 2221–2295.
[113] T.W. Webber, R.K. Chakkravorti, Pore and solid diffusion models for fixed-bed adsorbers, AlChE J. 20 (1974) 228–238.
[114] H.M.F. Freundlich, Over the adsorption in solution, J. Phys. Chem. 57 (1906) 385–471.
[115] X. Zhu, Y. Liu, C. Zhou, et al., A novel porous carbon derived from hydrothermal carbon for efficient adsorption of tetracycline, Carbon 77 (2014) 627–636.